

Drop-off-reinitiation triggered by EF-G-driven mistranslocation and its alleviation by EF-P

Kenya Tajima, Takayuki Katoh¹* and Hiroaki Suga¹*

Department of Chemistry, Graduate School of Science, The University of Tokyo, 7-3-1 Hongo, Bunkyo-ku, Tokyo 113-0033, Japan

Received September 22, 2021; Revised January 13, 2022; Editorial Decision January 14, 2022; Accepted February 07, 2022

ABSTRACT

In ribosomal translation, peptidyl transfer occurs between P-site peptidyl-tRNA and A-site aminoacyl-tRNA, followed by translocation of the resulting P-site deacylated-tRNA and A-site peptidyl-tRNA to E and P site, respectively, mediated by EF-G. Here, we report that mistranslocation of P-site peptidyl-tRNA and A-site aminoacyl-tRNA toward E and A site occurs when high concentration of EF-G triggers the migration of two tRNAs prior to completion of peptidyl transfer. Consecutive incorporation of less reactive amino acids, such as Pro and D-Ala, makes peptidyl transfer inefficient and thus induces the mistranslocation event. Consequently, the E-site peptidyl-tRNA drops off from ribosome to give a truncated peptide lacking the C-terminal region. The P-site aminoacyl-tRNA allows for reinitiation of translation upon accommodation of a new aminoacyl-tRNA at A site, leading to synthesis of a truncated peptide lacking the N-terminal region, which we call the ‘reinitiated peptide’. We also revealed that such a drop-off-reinitiation event can be alleviated by EF-P that promotes peptidyl transfer of Pro. Moreover, this event takes place both *in vitro* and in cell, showing that reinitiated peptides during protein synthesis could be accumulated in this pathway in cells.

INTRODUCTION

In ribosomal translation, nascent polypeptide chains are elongated by repeating the following three fundamental steps: (i) peptidyl transfer from the P-site peptidyl-tRNA onto the A-site aminoacyl-tRNA catalyzed by the peptidyl transferase center of ribosome, (ii) translocation of the resulting P-site deacylated-tRNA and A-site peptidyl-tRNA to the E site and P site, respectively, mediated by EF-G and (iii) accommodation of a new aminoacyl-tRNA onto the empty A site mediated by EF-Tu (1). Although the P-site peptidyl-tRNA is indispensable for the peptidyl transfer re-

action, the peptidyl-tRNA can be lost under certain conditions by drop-off from the ribosome, leading to truncation of peptides (2–5). For instance, elongation of inefficient substrates such as consecutive L-proline (Pro) residues (6–9) or some kinds of nonproteinogenic amino acids, e.g. β -, D- and N-methyl-amino acids, often suffers from peptidyl-tRNA drop-off (5). Moreover, since peptidyl-tRNA is stabilized at the P-site by interaction with the ribosomal exit tunnel, ones with short nascent peptides are more prone to drop-off due to insufficient interaction with the tunnel. Thus, drop-off is promoted by some macrolide antibiotics that hinder the interaction between the nascent peptide and the exit tunnel (10–14).

The dropped peptidyl-tRNA is eventually hydrolyzed by peptidyl-tRNA hydrolase (PTH) at the ester bond between peptide and 2'/3'-hydroxyl group of tRNA (15), ending up with generation of a truncated peptide lacking the C-terminal region, which we refer to as ‘drop-off peptide (DoP)’. On the other hand, the fate of the ribosome that has lost the peptidyl-tRNA is unclear due to the lack of comprehensive study of such a complex. Given the aminoacyl-tRNA as well as the mRNA still remain in ribosome, it is possible that the translation reinitiates by the migration of the aminoacyl-tRNA from A site to P site along with the mRNA, followed by accommodation of a new aminoacyl-tRNA onto the empty A site. In that case, a truncated peptide lacking the N-terminal region, which we call ‘reinitiated peptide (RiP)’, could be generated utilizing the remaining aminoacyl-tRNA as an N-terminal building block. Indeed, two related papers published by our group indicated such a possibility that not only peptidyl-tRNA drop-off but also RiP synthesis could occur (5,16). However, the mechanism how drop-off-reinitiation occurs to generate such RiPs remains elusive.

As for the translocation of the remaining aminoacyl-tRNA from A site to P site, EF-G would be the possible candidate responsible for such an event, similar to the case with the canonical translocation (17). Based on the fact that EF-G directly interacts with only A-site tRNA (18), we assumed that EF-G moves the A-site aminoacyl-tRNA toward the P site, and thereby the P-site peptidyl-tRNA is pushed out

*To whom correspondence should be addressed. Tel: +81 3 5841 8372; Fax: +81 3 5841 8372; Email: hsuga@chem.s.u-tokyo.ac.jp
Correspondence may also be addressed to Takayuki Katoh. Email: katoh@chem.s.u-tokyo.ac.jp

toward E site and eventually drops off, which we refer to as a ‘mistranslocation’ event. In order to verify this hypothesis, we have monitored mistranslocation events by increasing the EF-G concentration in expression of model peptides containing inefficient substrates, Pro or D-Ala, in a consecutive manner. As it has been previously reported that EF-P improves the efficiency of peptidyl transfer between consecutive Pro residues (7,8), the effect of EF-P on mistranslocation was also evaluated. In addition, the effect of length and sequence of nascent peptides, Shine-Dalgarno (SD)-like sequences in ORF, and other types of possible drop-off inducers such as RF2, RF3 and RRF are also evaluated.

MATERIALS AND METHODS

Preparation of cDNA templates, mRNA templates, Flexizymes and tRNAs

cDNA templates, mRNA templates, Flexizymes (dFx and eFx) and tRNAs used for translation and pre-charging of activated amino acids were prepared by PCR and *in vitro* transcription (see Supplementary Table S1A–H for their sequences). Template DNAs were prepared by extension of forward and reverse primer pairs, followed by PCR using forward and reverse PCR primers. The PCR products were extracted by phenol/chloroform, precipitated by ethanol, and used for transcription at 37°C for at least 3 h in a 100–2000 µl reaction mixture. For mRNA and Flexizymes, reaction mixture contained 40 mM tris(hydroxymethyl)aminomethane (Tris)-HCl (pH 8.0), 1 mM spermidine, 0.01% Triton X-100, 10 mM DTT, 30 mM MgCl₂, 5 mM NTPs, 30 mM KOH, 10% template DNA solution and 0.12 µM T7 RNA polymerase. For tRNAs, reaction mixture contained 40 mM Tris-HCl (pH 8.0), 1 mM spermidine, 0.01% Triton X-100, 10 mM DTT, 22.5 mM MgCl₂, 3.75 mM NTPs, 5 mM GMP, 22.5 mM KOH, 10% template DNA solution and 0.12 µM T7 RNA polymerase. The resulting RNA transcripts were treated with RQ1 DNase (Promega) for 1 h at 37°C and purified by 8% polyacrylamide gel containing 6 M urea.

Aminoacylation of tRNAs

Activated amino acids [L-lysine-3,5-dinitrobenzyl ester (Lys-DBE), L-asparagine-3,5-dinitrobenzyl ester (Asn-DBE), L-glutamate-3,5-dinitrobenzyl ester (Glu-DBE), L-leucine-3,5-dinitrobenzyl ester (Leu-DBE), L-isoleucine-3,5-dinitrobenzyl ester (Ile-DBE), L-phenylalanine-cyanomethyl ester (Phe-CME), L-methionine-3,5-dinitrobenzyl ester (Met-DBE), *N*-biotinylated L-phenylalanine-cyanomethyl ester (^{Bio}F-CME) and D-alanine-3,5-dinitrobenzyl ester (D-Ala-DBE)] were synthesized by previously reported methods (19,20). Aminoacylation was carried out at 0°C in a reaction mixture containing 50 mM HEPES-KOH (pH 7.5), 600 mM MgCl₂, 20% DMSO, 25 µM dFx or eFx, 25 µM tRNA and 5 mM activated amino acids. eFx was used for aminoacylation of Phe-CME and ^{Bio}F-CME and dFx for that of other amino acids. Reaction time was 2 h for all the activated amino acids. The aminoacyl-tRNAs were recovered by ethanol precipitation, and then pellet was washed twice with 70% ethanol containing 0.1 M sodium

acetate (pH 5.2), once with 70% ethanol and dissolved in 1 mM sodium acetate (pH 5.2).

Preparation of EF-P for *in vitro* translation reactions

Escherichia coli efp gene was cloned into a modified pET28a(+) vector that has PreScission protease recognition site instead of thrombin site (Supplementary Table S1I). *E. coli epmA* and *epmB* genes were cloned into pETDuet-1 vector. These vectors were co-introduced into *E. coli* Rosetta2 (DE3) pLysS. The cells were cultured in LB medium with 0.5 mM IPTG for 2 h at 37°C and lysed by sonication. The cell lysate was applied to HiTrap TALON crude column (Cytiva) to purify the histidine-tagged EF-P. The column was washed with buffer A (20 mM Tris-HCl (pH 8.0), 200 mM NaCl, 2 mM imidazole and 1 mM 2-mercaptoethanol) and then the histidine-tagged EF-P was eluted by buffer A containing 500 mM imidazole. Turbo3C protease was added to the eluate for cleaving the histidine-tag and dialyzed against the buffer A at 4°C overnight. The sample was applied on the HiTrap TALON crude column, and the flow-through and wash fractions were recovered as EF-P without histidine-tag. Then, the protein was concentrated by Amicon Ultra 10k centrifugal filter (Merck Millipore).

Expression of peptides in the reconstituted cell-free translation system

Peptides were expressed by utilizing modified FIT (Flexible *in vitro* translation system), in which unnecessary amino acids, aminoacyl-tRNA synthetases (aaRSs) and EF-P were withdrawn from the following mixture (See also supplementary Table S2 for the details of the translation conditions). The complete FIT system contains 2 µM template mRNA, 0.5 mM each 20 proteinogenic L-amino acids (Ala, Cys, Asp, Glu, Phe, Gly, His, Ile, Lys, Leu, Met, Asn, Pro, Gln, Arg, Ser, Thr, Val, Trp, Tyr), 2 mM ATP, 2 mM GTP, 1 mM CTP, 1 mM UTP, 20 mM creatine phosphate, 50 mM HEPES-KOH (pH 7.6), 100 mM potassium acetate, 12.8 mM magnesium acetate, 2 mM spermidine, 1 mM DTT, 1 mM tris(2-carboxyethyl)phosphine (TCEP), 0.1 mM 10-HCO-H4folate, 1.5 mg/ml *E. coli* tRNAs, 1.2 µM *E. coli* ribosome, 0.6 µM MTF, 2.7 µM IF1, 0.4 µM IF2, 1.5 µM IF3, 0.26 µM EF-G, 10 µM EF-Tu, 0.66 µM EF-Ts, 5 µM EF-P, 0.25 µM RF2, 0.17 µM RF3, 0.5 µM RRF, 4 µg/ml creatine kinase, 3 µg/ml myokinase, 0.1 µM inorganic pyrophosphatase, 0.1 µM T7 RNA polymerase, 0.73 µM AlaRS, 0.03 µM ArgRS, 0.38 µM AsnRS, 0.13 µM AspRS, 0.02 µM CysRS, 0.06 µM GlnRS, 0.23 µM GluRS, 0.09 µM GlyRS, 0.02 µM HisRS, 0.4 µM IleRS, 0.04 µM LeuRS, 0.11 µM LysRS, 0.03 µM MetRS, 0.68 µM PheRS, 0.16 µM ProRS, 0.04 µM SerRS, 0.09 µM ThrRS, 0.03 µM TrpRS, 0.02 µM TryRS and 0.02 µM ValRS. The concentration of EF-G was changed if necessary. To incorporate two consecutive D-Ala into a peptide, the FLPS2a peptide was expressed from mRNAS2 in the modified FIT system containing 50 µM D-Ala-tRNA^{GluE2}_{CGG}, only five amino acids (0.5 mM [¹²C]-Asp or 0.05 mM [¹⁴C]-Asp, 0.5 mM Gly, 0.5 mM Lys, 0.5 mM Met and 0.5 mM Tyr) and five aaRSs (0.13 µM AspRS, 0.09 µM GlyRS, 0.11 µM LysRS, 0.03 µM MetRS

and 0.02 μM TryRS). To distinguish whether drop-off is caused by mRNA context or nascent peptides, peptides were expressed from mRNAs utilizing the corresponding pre-charged aminoacyl-tRNAs in the modified FIT system containing only three amino acids (0.5 mM [^{12}C]-Asp or 0.05 mM [^{14}C]-Asp, 0.5 mM Met and 0.5 mM Tyr) and three aaRSs (0.13 μM AspRS, 0.03 μM MetRS and 0.02 μM TryRS). FLP3 was expressed from mRNA3 with 25 μM Leu-tRNA^{AsnE2}_{GAG} and 50 μM Lys-tRNA^{AsnE2}_{CUU}, or from mRNA4 with 25 μM Leu-tRNA^{AsnE2}_{CUU} and 50 μM Lys-tRNA^{AsnE2}_{GAG}. FLP2 was expressed from mRNA2 with 50 μM Lys-tRNA^{AsnE2}_{CUU}, or mRNA3 with 25 μM Lys-tRNA^{AsnE2}_{GAG} and 50 μM Lys-tRNA^{AsnE2}_{CUU}. FLP4 was expressed from mRNA5 with 25 μM Asn-tRNA^{AsnE2}_{GUU}, 50 μM Lys-tRNA^{AsnE2}_{CUU} and 25 μM Glu-tRNA^{AsnE2}_{CUC}, or from mRNA6 with 25 μM Asn-tRNA^{AsnE2}_{GAG}, 25 μM Lys-tRNA^{AsnE2}_{GAU}, 25 μM Glu-tRNA^{AsnE2}_{GAA} and 50 μM Lys-tRNA^{AsnE2}_{CUU}. FLP5 was expressed from mRNA6 with 25 μM Leu-tRNA^{AsnE2}_{GAG}, 25 μM Ile-tRNA^{AsnE2}_{GAU}, 25 μM Phe-tRNA^{AsnE2}_{GAA} and 50 μM Lys-tRNA^{AsnE2}_{CUU}, or from mRNA7 with 25 μM Leu-tRNA^{AsnE2}_{GUU}, 25 μM Ile-tRNA^{AsnE2}_{CUU}, 25 μM Phe-tRNA^{AsnE2}_{CUC} and 50 μM Lys-tRNA^{AsnE2}_{GAG}. In coding different amino acids in the initiation and elongation AUG codons, FLPM1(^{Bio}F, M) was expressed from mRNA1 with 100 μM ^{Bio}F-tRNA^{fMet}_{CAU} and 50 μM Met-tRNA^{AsnE2}_{CAU} without Met, MetRS and 10-HCO-H4folate or with 100 μM ^{Bio}F-tRNA^{fMet}_{CAU}, 0.5 mM Met and MetRS without 10-HCO-H4folate. In expression of representative peptides with various kinds of nascent peptide sequences prior to the three consecutive prolines, peptides were expressed with 12.5 μM ^{Bio}F-tRNA^{fMet}_{CAU} without 10-HCO-H4folate. The reaction mixture was incubated at 37°C for 20 min. In the identification of dropped peptidyl-tRNA or its nascent chain, the translation reaction mixture was incubated with 10 μM kanamycin (Nacalai tesque) for 5 min at 37°C, followed by incubation with 1 μM PTH for 10 min at 37°C, if necessary. In separation of the dropped peptidyl-tRNA and the peptidyl-tRNA trapped in the ribosome, the reaction mixture was mixed with equivalent volume of MeOH, centrifuged for 3 min at 13 000 rpm, and the supernatant and the precipitation was separated. The precipitation was re-resolved into 1 \times FIT buffer (20 mM Tris-HCl (pH 7.6), 50 mM KCl and 1 mM DTT), mixed with f.c. 12.8 mM EDTA, f.c. 10 μM kanamycin, f.c. 15.8 mM Mg(OAc)₂, f.c. 1 μM PTH and incubated at 37°C for 10, 30 or 60 min. Finally, the reaction mixture was incubated with f.c. 50 $\mu\text{g}/\text{ml}$ of RNase A (Funakoshi) for 30 min at 37°C if necessary.

In the identification by MALDI-TOF MS, the translation products were purified by anti-FLAG antibody if necessary. After addition of equal amount of 2 \times TBS buffer (100 mM Tris-HCl (pH 7.6) and 300 mM NaCl), the reaction mixture was incubated with anti-FLAG antibody agarose gel (Sigma) for 1 h at room temperature, followed by wash with 1 \times TBS buffer (50 mM Tris-HCl (pH 7.6) and 150 mM NaCl) twice and eluted with 0.1% TFA solution. Reaction mixture and elution were desalted with SPE C-tip (Nikkyo Technos) and eluted with 1.2 μl of 80% acetonitrile and 0.5% acetic acid solution containing 50% saturated (*R*)-cyano-4-hydroxycinnamic acid (Bruker Dalton-

ics). MALDI-TOF MS analysis was performed using ultrafleXtreme (Bruker Daltonics) in reflector positive mode. Peptide calibration standard II (Bruker Daltonics) was used for the external mass calibration.

For quantification of peptide yields, 0.5 mM [^{12}C]-Asp, [^{12}C]-Lys or [^{32}S]-Met in the FIT system were replaced with radio-labeled 0.05 mM [^{14}C]-Asp, 0.05 mM [^{14}C]-Lys or 0.868 μM [^{35}S]-Met. After incubation, reaction mixture was mixed with equal volume of 2 \times tricine-SDS-PAGE loading solution (0.9 M Tris-HCl, 8w/v% SDS, 30% glycerol, 0.001w/v% xylene cyanol, pH 8.45) and incubated at 95°C for 5 min. The solution was applied to the tricine-SDS polyacrylamide gel composed of 4% stacking gel and 15% separation gel and run for 40 min at 150 V with cathode buffer (0.1 mM Tris-HCl, 0.1 mM tricine, and 0.1w/v% SDS, pH 8.45) and anode buffer (0.2 mM Tris-HCl pH 8.9). After drying, the gel was exposed to an imaging plate for overnight and analyzed by Typhoon FLA 7000 (Cytiva).

In the identification and quantification by LC-ESI MS, proteins were precipitated by incubation of the reaction solution with equal volume of methanol on ice for 5 min, centrifuged at 13 000 rpm for 3 min, and centrifuged with 4 \times volume of 1% TFA at 13 000 rpm for 3 min. The resulting solution was injected to the LC-ESI MS (XevoTM G2-XS, Waters) assembled with Acquity UPLC BEH C18 column (1.7 μm , 300Å, 2.1 \times 150 mm, Waters) and eluted by gradient of water/acetonitrile containing 0.1% formic acid.

Profiling of nascent peptide sequence against peptidyl-tRNA drop-off and RiP generation

Nascent chain-dependent Pro/Gly incorporation efficiency was analyzed by an mRNA display-based profiling system. 1.2 μM mRNA conjugated with puromycin was translated in 2.5 μl of FIT system in the presence of 12.5 μM of ^{Bio}F-tRNA^{fMet}_{CAU} and in the absence of 10-HCO-H4folate, with 0.03, 0.26 or 10 μM EF-G and in the presence or absence of 5 μM EF-P. The reaction mixture was incubated at 37°C for 10 min, followed by incubation with f.c. 16.7 mM EDTA at 37°C for 5 min and reverse transcription by adding 1.72 μl of RT solution [0.73 mM dNTPs, 73.4 mM Tris-HCl (pH 8.3), 4.9 μM reverse primer, 29 mM KOH, 43.7 mM Mg(OAc)₂ and 14.6 U/ μl RTase (Promega)] at 42°C for 1 h. The reaction was quenched by addition of 0.5 μl of 100 mM EDTA and 0.55 μl of 0.2 M HCl. 0.5 μl of reaction mixture was aliquoted as 'Initial' fraction, diluted into 1 \times PCR mixture [50 mM KCl, 10 mM Tris-HCl (pH 9.0), 0.1% Triton X-100, 2.5 mM MgCl₂, 0.25 mM dNTPs and 0.25 μM of forward and reverse primer] by 100-fold. Remaining solution was incubated at room temperature for 10 min with 2.5 μl slurry of Dynabeads M-280 streptavidin (Veritas) washed by 1 \times TBST buffer (50 mM Tris-HCl (pH 7.6), 150 mM NaCl and 0.05% Tween-20) three times. After removal of supernatant, the Dynabeads was washed with 100 μl of 1 \times TBST and transferred to the new tube 10 times. The cDNA of ^{Bio}F-peptide-mRNA/cDNA conjugates were eluted by 1 \times PCR mix by incubation at 95°C for 5 min as 'Pull-down' fraction. After addition of Taq DNA polymerase into 1 \times PCR mixture, the amount of cDNA in the 'Initial' fraction and 'Pull-down' fraction was quantified by qPCR and amplified by PCR in optimum thermal cycles.

Amplified cDNAs were purified by phenol/chloroform extraction and ethanol precipitation. Adopter sequences for next generation sequencing were added to the purified cDNAs by PCR and purified by NucleoSpin Gel and PCR Clean-up (Macherey-Nagel). The purified cDNAs were sequenced by Miseq and Miseq reagent kit v3 (150 cycles) (Illumina). The ratio of a nascent peptide chain n in the 'Initial' or 'Pull-down' fraction, $P_{n(Ini)}$ and $P_{n(PD-/+)}$, enrichment of n in the presence or absence of EF-P through the selection process, $E_{n-/+}$, and incorporation enhancement by EF-P, W_n were calculated as following equations;

$$P_{n(Ini)} = \frac{Count_{n(Ini)}}{\sum_n^{8420} Count_{n(Ini)}}$$

$$P_{n(PD-/+)} = \frac{Count_{n(PD-/+)}}{\sum_n^{8420} Count_{n(PD-+)}}$$

$$E_{n-/+} = \log_2 \left(\frac{P_{n(PD-+)}}{P_{n(Ini)}} \right), \quad W_n = E_{n+} - E_{n-}$$

Preparation of plasmid coding YhhM and *efp* under an arabinose promoter

pBAD-P_{BAD}-YhhM-His₆ plasmid was prepared as follows (Supplementary Table S11). cDNAs of YhhM (purchased from Integrated DNA Technologies) were amplified by adopter PCR in order to add 15 nt homologous regions and purified by NucleoSpin Gel and PCR Clean-up (Macherey-Nagel). pBAD-HisA ColE1 ori plasmid (Thermo Fisher Invitrogen) were amplified with the same homologous region as those added to the cDNA of proteins by inversion PCR. PCR reaction contained 50% KODone premix (TOYOBO), 0.3 μM forward and reverse primers, and 1.00 ng/μl linear or circular template DNA. PCR reaction was performed at 94°C for 120 s, followed by repeat of 94°C for 10 s, 56°C for 30 s and 68°C for 60 s/1 kb. DNAs were purified by 1w/v% agarose gel electrophoresis. The resulting cDNA and linear plasmids were assembled by In-Fusion HD cloning kit (Takara bio). Transformation was carried out with 50 μl *E. coli* DH5α competent cells with 2.5 μl of In-Fusion reaction mixture, incubated on ice for 10 min, heat-shocked for 45 s at 42°C, incubated on ice for 2 min, and spread on LB plates containing 100 μg/ml ampicillin at 37°C for overnight. Single colonies were picked and cultivated in 4 ml LB broth with 100 μg/ml ampicillin at 37°C for overnight, and then plasmid was extracted by fast gene plasmid mini kit (Nippon Gene) and sequenced (Fasmaq). pBAD-P_{BAD}-YhhM-fh plasmid was prepared in the same procedure shown above.

pBAD-*efp*-p15A ori plasmid was prepared as follows. First, pBAD-*efp*-ColE1 ori plasmid was prepared by In-Fusion assembly (Takara bio) of an inversion PCR product of pBAD-HisA ColE1 ori plasmid (Thermo Fisher Invitrogen) and PCR product of *efp* gene from pET28a(+)-*efp* plasmid. Transformation was carried out with 50 μl *E. coli* DH5α competent cells with 2.5 μl of In-Fusion reaction mixture, following the same procedure as preparation of pBAD-P_{BAD}-YhhM-His₆ plasmid using ampicillin. Then a DNA fragment containing *araC*-P_{BAD} promoter-*efp* was amplified by PCR of the pBAD-*efp*-ColE1 ori plasmid

and a DNA fragment containing CmR-p15A ori was amplified by inversion PCR from pLysS plasmid, which were assembled by In-Fusion reaction. Transformation was carried out with 50 μl *E. coli* DH5α competent cells with 2.5 μl In-Fusion reaction mixture, following the same procedure as preparation of pBAD-P_{BAD}-YhhM-His₆ plasmid using 30 μg/ml chloramphenicol in LB. The recombinant plasmid was prepared and sequenced following the procedure shown above.

Complementation of *E. coli* cells lacking chromosomal *efp* gene by pBAD-*efp*-p15A ori plasmid

Expression and post-translational modification of EF-P was confirmed by using *E. coli* JW4107 strain lacking its chromosomal *efp* gene (*E. coli* Δ*efp*) (National BioResource Project-*E. coli*). *E. coli* Δ*efp* was transformed with pBAD-*efp*-p15A ori plasmid. The resulting *E. coli* Δ*efp*/pBAD-*efp*-p15A ori (*E. coli* Δ*efp*/+*efp*) was cultivated in 0.5 L LB with 50 μg/ml kanamycin and 30 μg/ml chloramphenicol for 4.5 h at 37°C and expression of *efp* gene was induced by 0.02% L-arabinose for 4 h at 37°C. The *E. coli* pellet was recovered by centrifugation at 8000 rpm for 10 min, flash-frozen and stored at -80°C. The pellet was resuspended with lysis buffer (20 mM Tris-HCl (pH 7.4), 200 mM NaCl, 1 mM DTT and 0.1 mM PMSF), sonicated and centrifuged at 15 000 g for 10 min. The supernatant was filtered by Minisart NML GF and Minisart NML hydrophile (Sartorius) and applied to HiTrap TALON crude (Cytiva). Then, EF-P was eluted with imidazole gradient and digested by 100 ng/μl Glu-C proteinase (Sigma) in 50 mM Tris-HCl (pH 8.0). After methanol precipitation and trifluoroacetic acid precipitation, the solution was analyzed by LC-ESI MS (Xevo™ G2-XS, Waters) assembled with Acquity UPLC BEH C18 column (1.7 μm, 300Å, 2.1 × 150 mm, Waters) and eluted by gradient of water/acetonitrile containing 0.1% formic acid.

Expression and purification of YhhM-fh in *E. coli* Δ*efp* and *E. coli* Δ*efp*/+*efp*

After transformation of *E. coli* Δ*efp* strain and *E. coli* Δ*efp*/+*efp* strain by pBAD-P_{BAD}-YhhM-fh plasmid, the resulting single colony was pre-cultivated in 2 ml of LB with 100 μg/ml ampicillin and 50 μg/ml of kanamycin for the *E. coli* Δ*efp* strain and with additional 30 μg/ml chloramphenicol for *E. coli* Δ*efp*/+*efp* strain at 37°C for overnight. The preculture broth was added to 100 ml of LB broth containing the same antibiotics, cultivated at 37°C for 4 h, and induced with f.c. 0.02% L-arabinose at 37°C for 4 h. *E. coli* pellet was recovered by centrifugation at 8000 rpm for 10 min, flash-frozen and stored at -80°C. The pellet was resuspended with lysis buffer (20 mM Tris-HCl (pH 7.4), 200 mM NaCl, 1 mM DTT and 0.1 mM PMSF), sonicated and centrifuged at 15 000 g for 10 min. The supernatant was applied to pre-equilibrated 1 ml slurry of His Super Flow (Cytiva) and eluted by imidazole gradient. The fractions containing YhhM-fh were analyzed by glycine-SDS-PAGE. The band corresponding to YhhM-fh was eluted from the gel and purified by PD10 (Cytiva) in order to remove DTT. Then, YhhM-fh was further purified by anti-FLAG M2

agarose gel (Sigma) and concentrated by Amicon Ultra 10k MW cut-off (Merck Millipore).

Sequence identification of YhhM-fh digested with Lys-N by LC-ESI MS/MS

0.67 μg of YhhM-fh expressed in *E. coli* Δefp and 1.3 μg of YhhM-fh expressed in *E. coli* $\Delta\text{efp}/+\text{efp}$ was digested by 0.027 $\mu\text{g}/\mu\text{l}$ Lys-N (Thermo Fisher Invitrogen) with 0.05 M NH_4HCO_3 (pH 8.2) in 30 μl reaction mixture at 37°C for 16 h. The reaction mixtures were desalted by SPE C-tip (Nikkyo Technos) and eluted with 30 μl of 80% acetonitrile with 0.5% acetic acid solution. The eluates were analyzed by LC-ESI MS^E and LC-ESI MS/MS (Xevo™ G2-XS, Waters) assembled with Acquity UPLC BEH C18 column (1.7 μm , 300 Å, 2.1 \times 150 mm, Waters) and eluted by gradient of water/acetonitrile containing 0.1% formic acid. First, the parent ions were screened by MS^E (Data-Independent Acquisition, DIA) method. *m/z* values corresponding to parent peptide fragments were screened by UniFi software (Waters). In order to sequence the N-terminal fragments, parent ions were fragmented by MS/MS mode. In MS/MS analysis, parent ions having a specific *m/z* value was selected by the quadrupole and fragmented by collision-induced dissociation using ramping of collision energy from 10 to 40 V. The daughter ions were identified by MassLynx software (Waters) after deconvolution of raw MS/MS spectra.

RESULTS

Peptidyl-tRNA drop-off and reinitiated peptide synthesis upon incorporation of consecutive Pro residues

To observe the EF-G-driven mistranslocation event, we conducted *in vitro* translation of mRNAs into model peptides containing consecutive Pro residues with titration of EF-G concentration. mRNA2 encodes a model full-length peptide FLP2 that have three consecutive Pro, whereas mRNA1 encodes a negative control peptide FLP1 that has three Gly in place of Pro (Figure 1A). Since peptidyl transfer between consecutive Pro is extremely inefficient due to the poor abilities in peptidyl donor and acceptor (9,21,22), we expected to observe drop-off-reinitiation in translation of mRNA2 but not in mRNA1. Peptides were radioisotope-labelled by incorporating [¹⁴C]-aspartic acid (Asp, D) in the C-terminal FLAG sequence (Asp-Tyr-Lys-Asp-Asp-Asp-Asp-Lys) for quantification of product bands in tricine SDS-PAGE by autoradiography. In translation of mRNA1, only the full-length product FLP1 was observed [Figure 1B, Supplementary Figure S1A: mRNA1, EF-P (–)], whereas two products were observed in mRNA2: the full-length FLP2 and the reinitiated peptide RiP2 derived from truncation between the second and third Pro residues [Figure 1B, Supplementary Figure S1A: mRNA2, EF-P (–), grey and red, respectively]. To further confirm the identity of these peptides, mRNA1 and mRNA2 were translated with [¹²C]-cold Asp instead of [¹⁴C]-Asp, and analyzed by MALDI-TOF mass spectrometry (MS) and MALDI-TOF MS/MS, in which only FLP1 was detected in the translation of mRNA1, whereas both FLP2 and RiP2 were detected in the translation of mRNA2 (Figure 2A, B: mRNA1 and mRNA2). The drop-off peptide DoP2 was not

detected because PTH is not added in this analysis and thus DoP2 should not be released from the tRNA. These results indicate that the mistranslocation event occurs with fMet-Lys-Lys-Lys-Pro-tRNA at P site and Pro-tRNA at A site; the former dropped off and the latter migrated to P site, then translation is reinitiated from the Pro-tRNA to generate the RiP2.

In order to analyze the effect of the number of consecutive Pro residues on mistranslocation, translation of mRNA1 and mRNA2, expressing the full-length FLPS1 and FLPS2 containing one and two consecutive Pro residues, respectively, was conducted, and the products were compared to those of mRNA1 and mRNA2 (Figures 1A, B, 2A, Supplementary Figure S1A). An intense peak of RiPS2 along with FLPS2 were observed for mRNA2, similar to the products of RiP2 and FLP2 expressed from the mRNA2 template. On the other hand, the mRNA1 template produced only the full-length peptide FLPS1. This indicates that two consecutive incorporations of Pro is less efficient than its single incorporation, promoting the RiP synthesis. In the case of mRNA2 translation, the expression level of the full-length FLPS2 dramatically decreased at higher concentrations of EF-G [Figure 1B: mRNA2, EF-P (–)], indicating that EF-G indeed triggers peptidyl-tRNA drop-off and thereby inhibits the usual level of FLPS2 synthesis. The expression level of RiPS2 increased at such high concentrations of EF-G, indicating that EF-G mediates the migration of A-site aminoacyl-tRNA to P site for the reinitiation. Consequently, the ratio of the RiPs increased in an EF-G concentration-dependent manner. A similar tendency was also observed in the translation of mRNA2, in which the ratio of RiP2 increases at higher concentrations of EF-G [Figure 1B: mRNA2, EF-P (–)]. These results show that both inefficient peptidyl transfer (i.e. consecutive Pro) and frequent translocation (i.e. high EF-G concentration) lead to the drop-off-reinitiation event. Since not only EF-G but also RF2, RF3 and RRF have been previously suggested to induce peptidyl-tRNA drop-off (23–25), we also titrated them in the translation of mRNA2; however, no significant enhancement in the RiP2 synthesis was observed with higher concentration of those factors (Figure 1C). Thus, we concluded that RF2, RF3 and RRF were not involved in the drop-off-reinitiation event.

Next, we analyzed the effect of EF-P on the drop-off-reinitiation. It has been previously reported that EF-P recognizes a specific D-arm motif found in the tRNA^{Pro} isoacceptors and accelerates peptidyl transfer in the elongation of Pro (7,8,26). EF-P is also involved in alleviation of translocation defects arising from miscoding and frameshifting (27,28). In translation of mRNA2, EF-P greatly enhanced the expression level of FLP2 and reduced that of RiP2 (Figure 1B: mRNA2, 2.2 μM of FLP2 and 0.1 μM RiP2 in the presence of EF-P and 0.26 μM EF-G, while 0.17 μM of FLP2 and 0.14 μM RiP2 in the absence of EF-P and presence of 0.26 μM EF-G), showing that efficient peptidyl transfer could suppress the drop-off-reinitiation. Since EF-P requires β -lysinylation at Lys34 for its full activity, we also evaluated the effect of using an unmodified EF-P in translation of mRNA2 into FLP2 and RiP2 (Supplementary Figure S2). Consequently, even the unmodified EF-P could suppress RiP synthesis and enhance the ratio

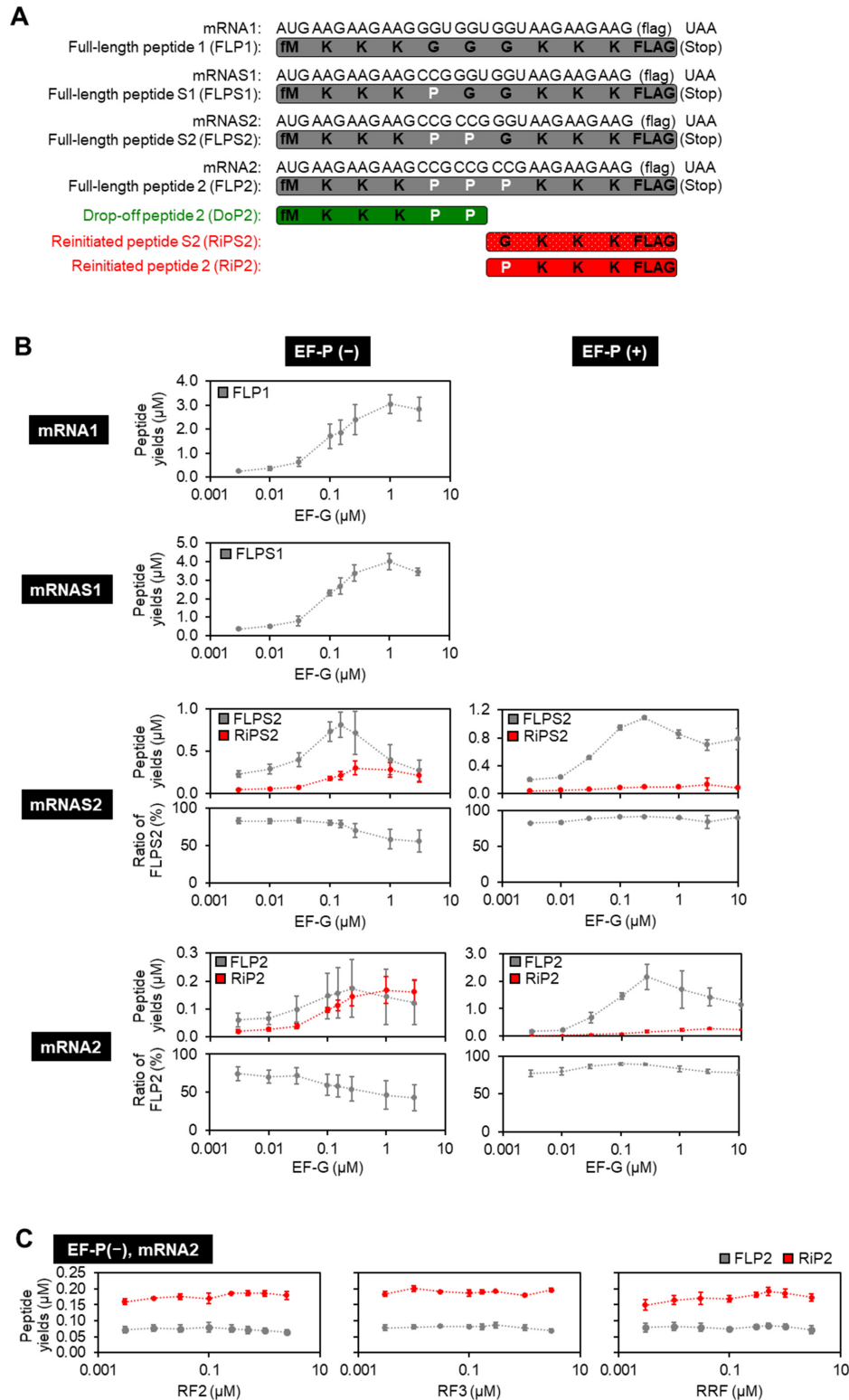


Figure 1. Quantification of full-length and reinitiated peptides in incorporation of consecutive Pro residues. (A) mRNA and expressed peptide sequences: full-length peptide (FLP1, FLPS1, FLPS2 and FLP2), drop-off peptide (DoP2), and reinitiated peptide (RiP2). (B) Titration of EF-G in translation of mRNA1, mRNAS1, mRNAS2 and mRNA2 in the absence or presence of 5 μ M EF-P. Expressed peptides were labelled by [14 C]-Asp and quantified by autoradiography. Expression levels of FLP1, FLPS1, FLPS2, FLP2, RiPS2 and RiP2 are shown. The ratio of FLPS2 or FLP2 was defined as (the yield of FLPS2 or FLP2)/(the sum of yields of translation products). Since only FLPs were observed in translation of mRNA1 and mRNAS1, ratio of them were omitted. $n = 3$. (C) Titration of RF2, RF3 and RRF in translation of mRNA2 in the absence of EF-P. Yields of FLP2 and RiP2 were quantified by autoradiography. $n = 3$.

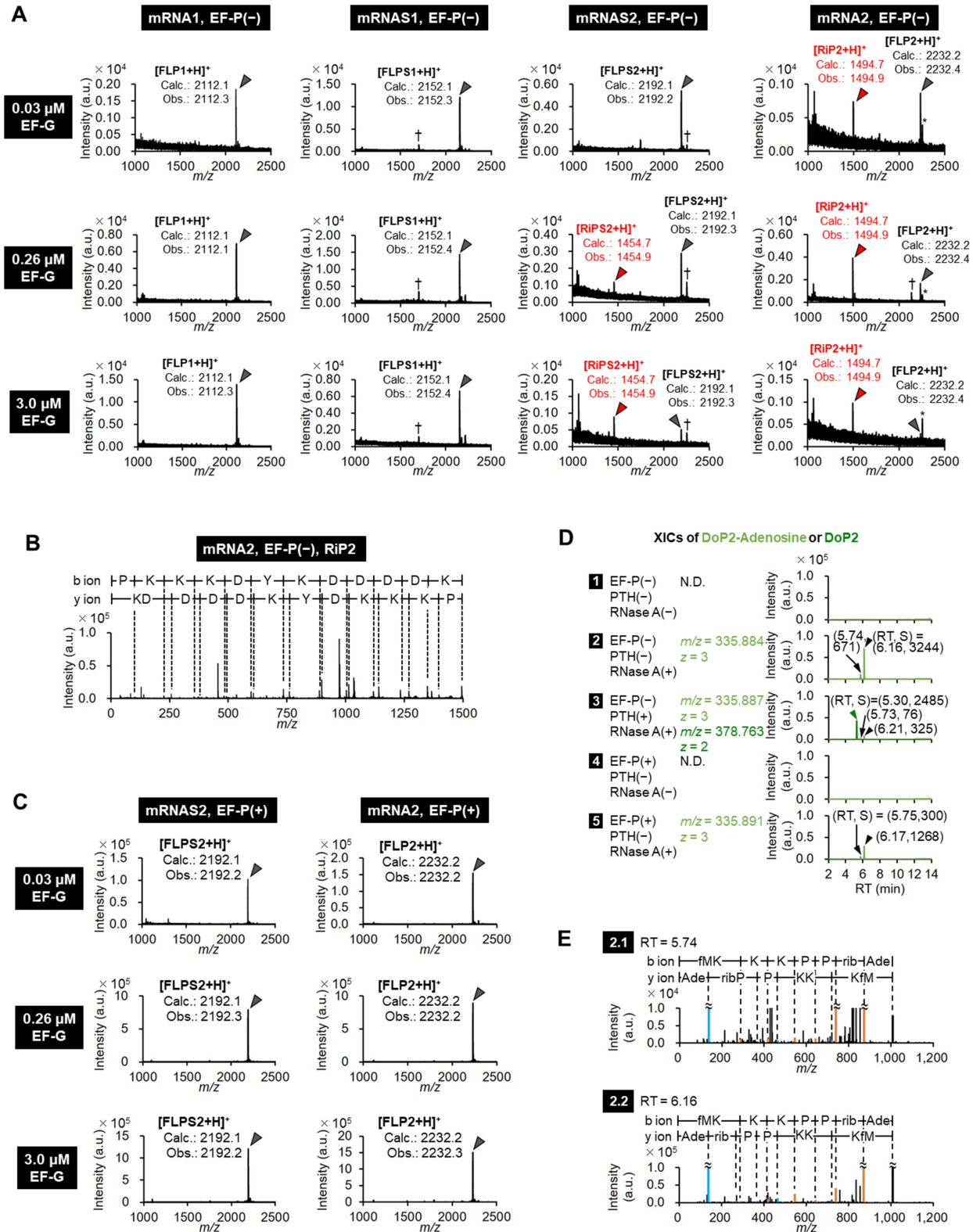


Figure 2. Mass spectrometric analysis of full-length and truncated peptides in incorporation of consecutive Pro. (A) Identification of translation products by MALDI-TOF MS. Peptides were expressed with 0.03, 0.26 or 3.0 μM EF-G in the absence of EF-P. *: Na⁺ or K⁺ adduct peaks, †: Unidentified peaks. ‘Calc.’ and ‘Obs.’ indicate calculated and observed *m/z* values, respectively. (B) MALDI-TOF MS/MS identification of RiP2 generated in the translation of mRNA2 with 0.26 μM EF-G. (C) Identification of translation products expressed in the presence of 5 μM EF-P by MALDI-TOF MS. (D) LC-ESI MS identification of drop-off DoP2-tRNA^{Pro} derivatives treated with PTH and/or RNase A. Their extracted ion current chromatograms (XICs) were extracted by using the indicated *m/z* values. Concentrations of EF-P, PTH and RNase A were 5 μM, 1 μM and 50 μg/ml, respectively. Black arrow-heads indicate the peaks of DoP2-Adenosine, and a green arrow-head DoP2. (E) Deconvoluted LC-ESI MS/MS spectra of DoP2-Adenosine observed at RT = 5.74 min (2.1) and RT = 6.16 min (2.2) in the XIC 2 in Figure 2D.

of FLP, although its effect was weaker than the use of β -lysylated EF-P. This result indicates that the EF-P in the E site blocks the movement of the P-site peptidyl-tRNA to the E site, thereby suppressing peptidyl-tRNA drop-off. Both the acceleration of peptidyl transfer and the blocking of the movement of the P-site tRNA should contribute to the suppression of drop-off-reinitiation event.

Since not only Pro but also some kinds of nonproteinogenic amino acids, such as D-amino acids, cause inefficient peptidyl transfer reaction, we also evaluated the frequency of reinitiated peptide synthesis in two-consecutive incorporation of D-Ala into FLPS2a using mRNAS2 (Figure 3A). D-Ala was pre-charged onto an artificial suppressor tRNA, tRNA^{GluE2}_{CGG}, using flexizyme and introduced at CCG codons by means of genetic code reprogramming in a reconstituted translation system that lacks Pro. As a result, two types of reinitiated peptides, RiPS1a and RiPS2, were detected by MALDI-TOF MS (Figure 3B). RiPS1a and RiPS2 could not be separated on a tricine-SDS-PAGE gel due to the only single amino acid difference between them. Therefore, the sum of the expression level of these two peptides were estimated and compared to that of the full-length peptide, FLPS2a (Figure 3C, D). Consequently, the ratio of the RiPs significantly increased at higher EF-G concentrations. This tendency was consistent with that of consecutive Pro incorporation.

Detection of drop-off peptides

In order to detect the drop-off peptide, translation of mRNA2 was conducted in the presence of [¹⁴C]-Lys so that all of FLP2, DoP2 and RiP2 were radio-labeled, and then PTH (15) was added after 20-min translation to remove tRNA moiety of the dropped peptidyl-tRNA (DoP2-tRNA). We observed a band corresponding to DoP2 at high PTH concentrations (Supplementary Figure S1B, DoP2), while the intensity of a band corresponding to DoP2-tRNA decreased by elevation of the PTH concentrations (Supplementary Figure S1B: DoP2-tRNA). However, the band of DoP2-tRNA did not completely disappear at 1 μ M or above. We hypothesized that this is because unhydrolyzed [¹⁴C]-Lys-tRNA^{Lys} or peptidyl-tRNA protected from PTH by stalled ribosome overlapped on this band (29). In order to confirm this, not only PTH but also RNase A were added after 20-min translation, by which the PTH-sensitive band completely disappeared (Supplementary Figure S1C). This is probably because RNase A could decompose both dropped and ribosome-protected peptidyl-tRNAs. The band at the bottom that was observed in the presence of RNase A should be a peptidyl-adenosine (DoP2-adenosine) derived from the DoP2-tRNA (Supplementary Figure S1C: 50 μ g/ml RNase A). Then, the DoP2 was also analyzed by LC-ESI MS (Figure 2D). Addition of RNase A gave two peaks bearing the same m/z values (Figure 2D, 2, $m/z = 335.844$, relative peak intensities were 671 and 3244, indicated by black arrow-heads), both of which were identified as DoP2-adenosine molecules by LC-ESI MS/MS analysis (Figure 2E). In the presence of PTH as well as RNase A, the intensity of DoP2-adenosine decreased by 10-fold, and instead a peak corresponding to DoP2 appeared (Figure 2D, 2 and 3: Relative peak intensity

of DoP2-adenosine decreased from 671 to 76 at RT = 5.74 min, and from 3242 to 325 at RT = 6.15 min. The intensity of DoP2 was 2485.). The expression of DoP2-adenosine was significantly suppressed in the presence of EF-P (Figure 2D: 2 and 5, relative peak intensity change from 671 to 300 at RT = 5.74 min, and from 3244 to 1268 at RT = 6.15 min).

Effects of length and sequence of nascent peptides on mis-translocation

As explained above, the length of nascent peptide of P-site peptidyl-tRNA should be one of critical determinants of drop-off frequency. Therefore, we examined different lengths of nascent peptides with EF-G titration (Figure 4A: FLPL1–4). Peptides were [¹⁴C]-Asp-labelled in the C-terminal FLAG, and analyzed by tricine-SDS-PAGE and autoradiography (Figure 4B, C). In the absence of EF-P, the expression of FLPL1–4 yielded the corresponding full-length peptides along with RiP2 (Figure 4B: FLPL1–4, grey bars; RiP2, red bars). At the high EF-G concentration (3 μ M), shorter peptides, FLPL3 and 4, exhibited low FLPL ratios [FLPL3/(FLPL3 + RiP2) and FLPL4/(FLPL4 + RiP2), respectively], indicating more frequent peptidyl-tRNA drop-off due to their insufficient stabilization via interaction with the exit tunnel. On the other hand, longer peptides, FLPL1 and 2, exhibited significantly higher FLPL ratios. (Figure 4C: ratio of FLPL1, 2, 3 and 4 were 75, 78, 44 and 43% at 3 μ M EF-G). The identities of FLPL1–4 and RiP2 were also confirmed by MALDI-TOF MS using non-radio-labeled peptides (Figure 4D).

It has been also reported that certain nascent peptide sequences interact with the exit tunnel so strongly as to induce ribosomal stalling and slow down the peptidyl transfer (30). There is also an argument for a possibility that purine-rich Shine-Dalgarno (SD)-like mRNA ORF sequences interact with the pyrimidine-rich anti-SD sequence of 16S rRNA to cause ribosome stalling (31,32). Therefore, we next analyzed the effect of such nascent peptide and corresponding mRNA sequences. mRNA2 is translated into FLP2 containing positively-charged Lys-Lys-Lys residues prior to the Pro-Pro-Pro, which is encoded by a purine-rich SD-like sequence (AAGAAGAAG in Figure 5A). On the other hand, mRNA6 is translated into FLP5 bearing hydrophobic residues (Leu-Ile-Phe) encoded by non-SD-like pyrimidine-rich codons (CUCAUCUUC) followed by three consecutive Pro. Translation of mRNA6 into FLP5 yielded only small amount of RiP2 [Figure 5C, Supplementary Figure S1E: lane 7, Figure 5E: mRNA6/FLP5, EF-P(–)], whereas that of mRNA2 into FLP2 yielded a noticeable amount of RiP2 [Figure 5C, Supplementary Figure S1E: lane 3, Figures 1B, 5E: mRNA2/FLP2, EF-P(–)]. Another polar nascent peptide encoded by an SD-like sequence, AACAAGGAG/Asn-Lys-Glu (mRNA5/FLP4), also resulted in significantly higher amount of RiP2 synthesis compared with another hydrophobic nascent peptide encoded by a non-SD-like sequence, CUCCUCCUC/Leu-Leu-Leu (mRNA3/FLP3) [Figure 5C, Supplementary Figure S1E: lane 5 and 1, respectively, Figure 5E: mRNA5/FLP4 and mRNA3/FLP3, EF-P(–)]. We also confirmed that the ratio of reinitiated peptide increased at higher EF-G concentra-

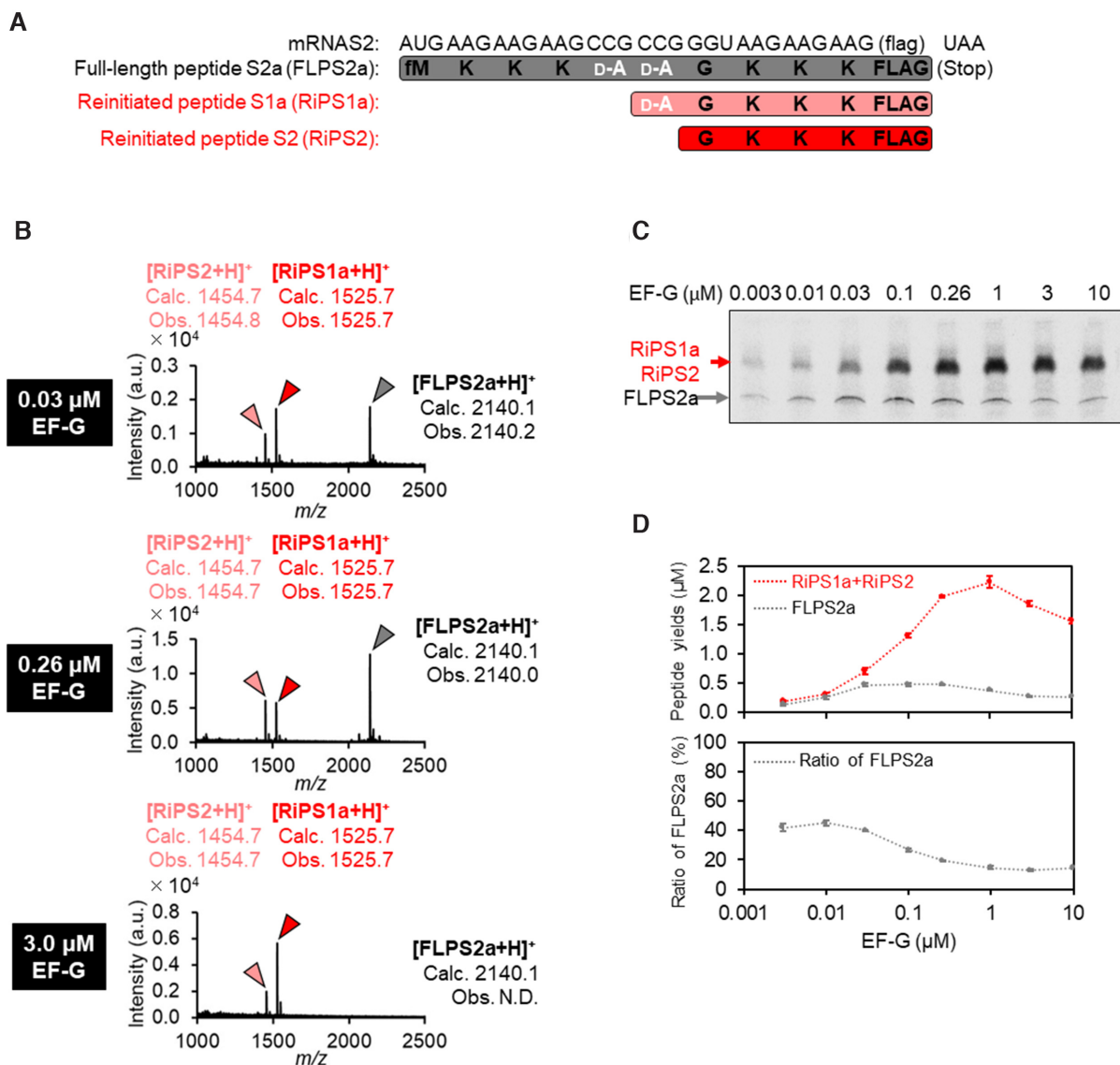


Figure 3. Mass spectrometric analysis and quantification of full-length and reinitiated peptides in incorporation of two consecutive D-alanines. (A) mRNA and expressed peptide sequences: full-length peptide (FLPS2a) and reinitiated peptides (RiPS1a and RiPS2). (B) Identification of translation products by MALDI-TOF MS. Peptides were expressed with 0.03, 0.26 or 3.0 μ M EF-G. ‘Calc.’ and ‘Obs.’ indicate calculated and observed m/z values, respectively. (C) Titration of EF-G concentration in translation of mRNAS2. RiPS1a and RiPS2 could not be separated on the tricine-SDS-PAGE gel due to the only single amino acid difference between them. (D) Titration of EF-G concentration in translation of mRNAS2. Expressed peptides were radioisotope-labelled by [¹⁴C]-Asp in the C-terminal FLAG sequences, separated by tricine-SDS-PAGE, and quantified by autoradiography. Yields of peptides were quantified by autoradiography. $n = 3$.

tions [Figure 5F, mRNA6/FLP5, EF-P(-)] and decreased in the presence of EF-P [Figure 5D, E, F: mRNA3/FLP3, mRNA2/FLP2, mRNA5/FLP4 and mRNA6/FLP5, EF-P(+)]. These results indicate that polar amino acids encoded by such SD-like mRNA sequences, mRNA2/FLP2 and mRNA5/FLP4, induce the mistranslocation event. However, it was yet unclear which is more or the most critical factor, mRNA context or peptide sequence. Therefore, we changed the relationship between codons and amino acids by means of genetic code reprogramming (33) (Figure 5G), by which FLP3 bearing hydrophobic Leu-Leu-Leu was expressed from both the non-SD-like mRNA3 and SD-like mRNA4 (Figure 5C: lane 1 and 2, Figure 5E, H) and

FLP5 with hydrophobic Leu-Ile-Phe was expressed from both the non-SD-like mRNA6 and SD-like mRNA7 (Figure 5C: lanes 7 and 8, Figure 5E, H). Ribosomal syntheses of FLP3 or FLP5 bearing the hydrophobic residues yielded the full-length peptide regardless of the mRNA context. Likewise, regardless of the context of mRNA template, ribosomal syntheses of FLP2 and FLP4 bearing the polar Lys-Lys-Lys and Asn-Lys-Glu residues, respectively, resulted in a noticeable amount of truncated RiP2 along with the full-length peptides (Figure 5C: lanes 3, 4, 5 and 6, Figure 5E, H). These results showed that induction of the drop-off-reinitiation event could be dictated by the peptide sequence rather than the mRNA context (Figure 5B).

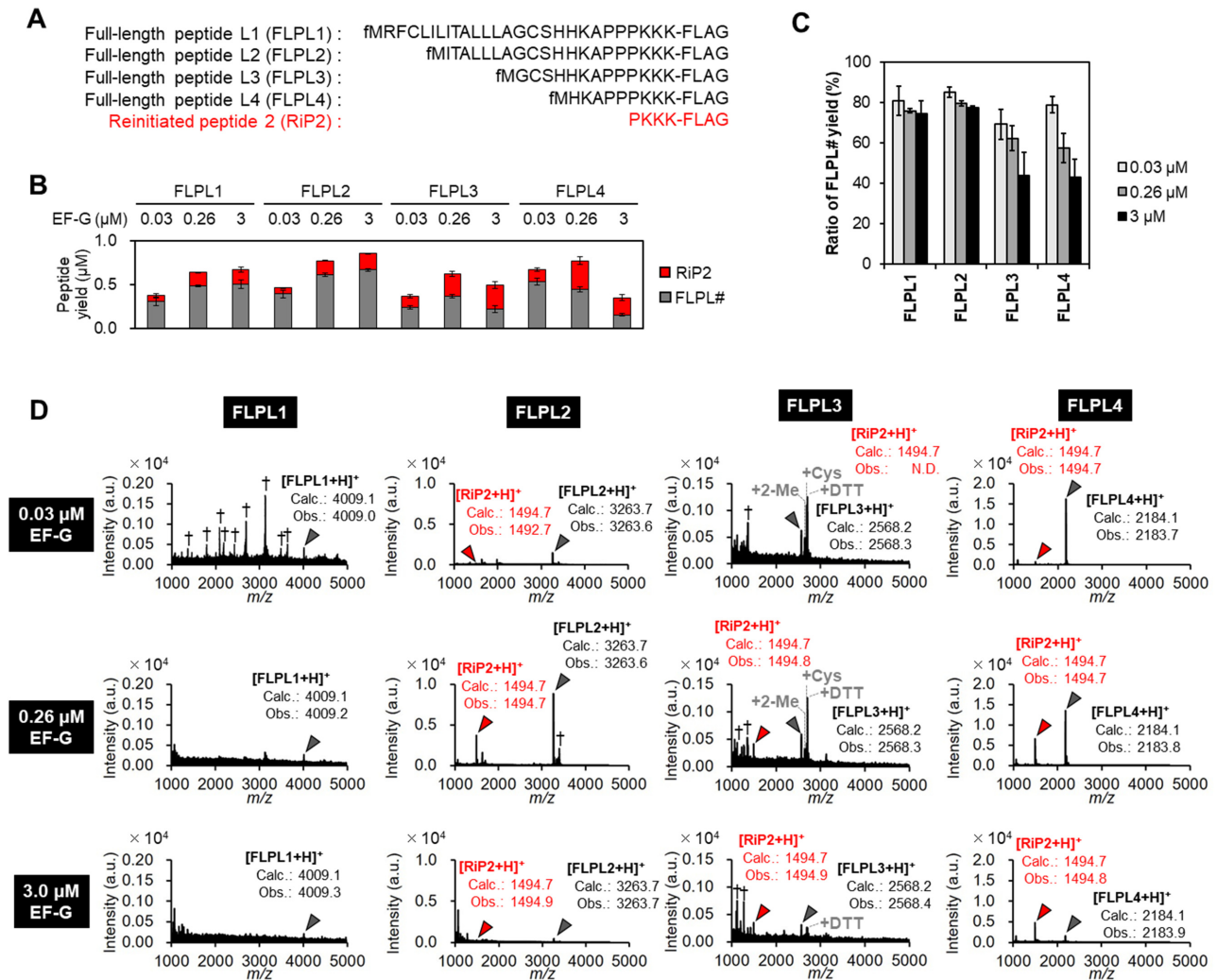


Figure 4. Effect of the length of nascent peptide chain on mistranslocation event. (A) Peptide sequences used in this analysis. The N-terminal region of NlpC protein containing a PPP motif was fused with KKK and FLAG peptide. FLPL1: The complete N-terminal peptide sequence derived from NlpC. FLPL2–4: Shortened variants of FLPL1. (B) Translation yields of FLPL1–4 and RiP2 in titration of EF-G in the absence of EF-P. Peptides were labeled by [¹⁴C]-Asp and quantified by autoradiography, $n = 3$. (C) Ratios of full-length peptides FLPL1–4. The ratios were calculated as (yield of FLPL#)/[(yield of FLPL#) + (yields of RiP2)] using the values obtained in (B), $n = 3$. (D) Identification of the translation products by MALDI-TOF MS. Peptides were expressed with 0.03, 0.26 or 3.0 μM EF-G in the absence of EF-P for 20 min. Grey arrowheads: FLPL1–4, red arrowheads: RiP2, *, Na⁺ or K⁺ adduct peaks, †: unidentified peaks. +2-ME, +Cys and +DTT are 2-mercaptoethanol, cysteine and dithiothreitol adducts, respectively. ‘Calc.’ and ‘Obs.’ indicate calculated and observed m/z values, respectively. N.D.: not detected.

We propose a possibility that the electrostatic interaction between polar/charged nascent peptides and the exit tunnel may hold the peptidyl-tRNA at an inactive position in the peptidyl transferase center (PTC) and cause inefficient peptidyl transfer reaction.

Comprehensive analysis of nascent peptide sequences that induce drop-off-reinitiation

To further explore nascent peptide sequences that induce drop-off-reinitiation, we applied a means of an mRNA display-based profiling (34). We constructed an mRNA library bearing 1–3 NNN random codons preceding three consecutive CCG Pro codons followed by a linker sequence (Figure 6A: a mixture of mRNA libraries 1, 2 and 3), where the N-terminal N-biotinyl-phenylalanine (BioF) was

installed by the initiation reprogramming. The peptide library expressed from this mRNA library was designed to contain 8,420 different peptide sequences to which 3' end of the mRNA library was ligated via a puromycin linker for the formation of peptide-mRNA fusion (Figure 6B). We then translated the mRNA sequences with 0.03, 0.26 or 10 μM of EF-G in the absence or presence of EF-P, producing the respective mRNA-peptide fusions followed by reverse-transcription. Since only the full-length peptide-mRNA fusions should have the N-terminal BioF, they were selectively recovered by streptavidin beads via the N-terminal biotin. Thereby, the deep sequencing of such cDNAs would reveal the populations of fully expressed peptide sequences.

By processing the sequencing data, proportion of a particular peptide sequence ‘ n ’ in the initial library was estimated as $P_n(\text{Ini})$, and that in the pulled-down library ob-

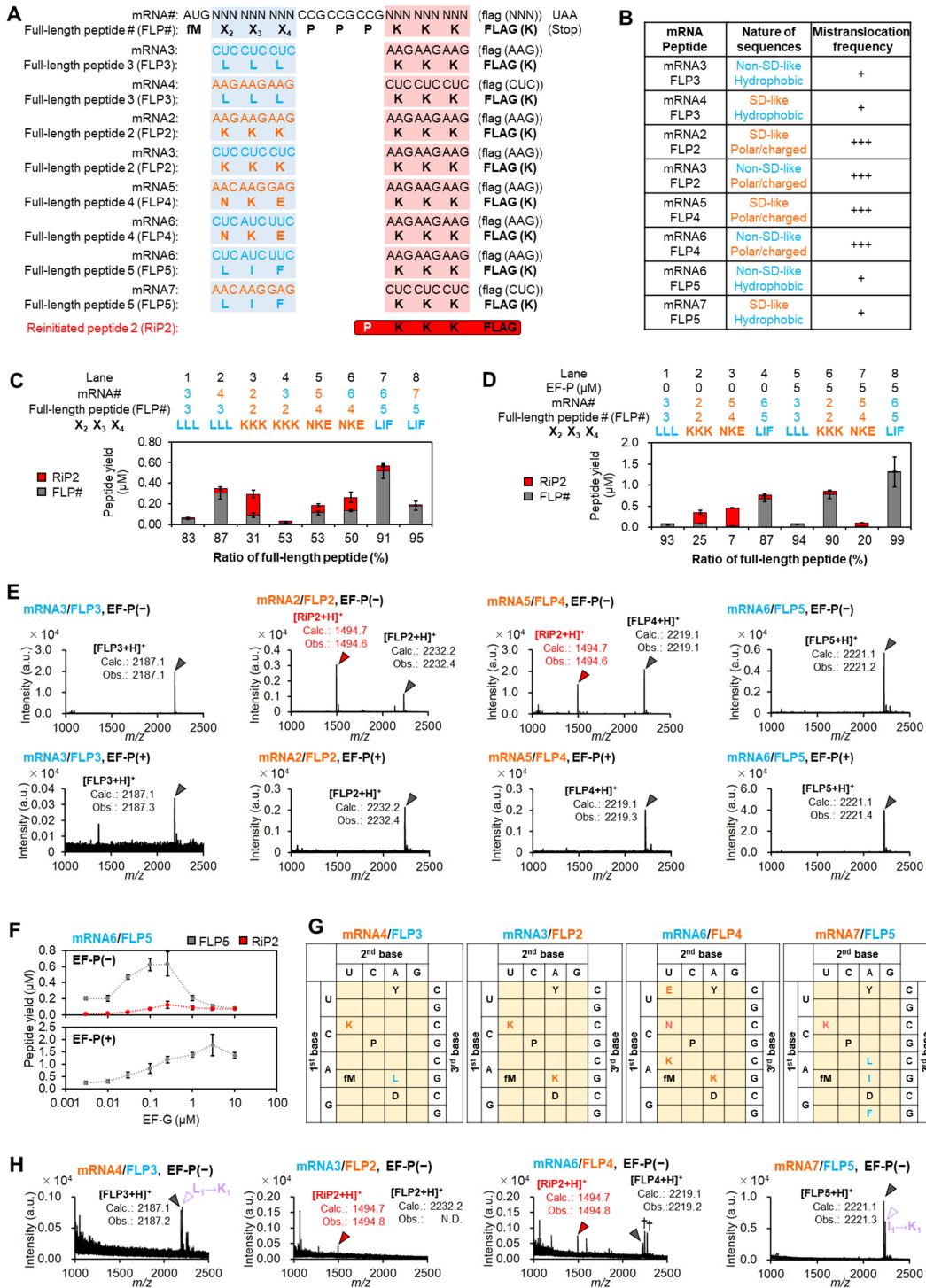


Figure 5. Drop-off-reinitiation caused by nascent peptide chain sequences. (A) Peptides (FLP2–5) and the corresponding mRNAs (mRNA2–7). The canonical genetic code assigns hydrophobic amino acids (sky-blue) to pyrimidine-rich codons (sky-blue), and polar amino acids (orange) to purine-rich codons (orange). Reprogrammed genetic codes (see also G) assign hydrophobic amino acids (sky-blue) to purine-rich codons (orange), and polar amino acids (orange) to pyrimidine-rich codons (sky-blue). The lysine residues that appear in the FLAG sequences are assigned to the codons indicated in parentheses. (B) Relationship between mistranslocation frequency and the nature of nascent peptide sequences/mRNA sequences. (C, D) Expression of the peptides (FLP2–5) from using the canonical or reprogrammed genetic codes in the absence (C: lanes 1–8, D: lanes 1–4) or presence of EF-P (D: lanes 5–8). $n = 3$. (E) Identification of the peptides expressed in (D). Grey arrowheads indicate peaks of FLP#s, and red arrowheads RiP2. ‘Calc.’ and ‘Obs.’ indicate calculated and observed m/z values, respectively. (F) Titration of EF-G in translation of mRNA6 to express FLP5 in the absence (top) and presence (bottom) of 5 μ M EF-P. $n = 3$. (G) Reprogrammed codon tables used in translation of mRNA4 to FLP3, mRNA3 to FLP2, mRNA6 to FLP4 and mRNA7 to FLP5. (H) MALDI-TOF-MS identification of the peptides expressed in (C), lanes 2, 4, 6 and 8. Grey arrowheads indicate peaks of full-length peptides, and red ones peaks of reinitiated peptides. Purple open triangles indicate peaks corresponding to the FLP bearing L-to-K or I-to-K misincorporation. N.D.: not detected.

tained in the absence or presence of EF-P was estimated as $P_{n(PD-)}$ or $P_{n(PD+)}$, respectively. Then, enrichment of the peptide sequence n after pull-down compared to the initial library was evaluated as E_{n-} and E_{n+} , which were calculated by $\log_2 [P_{n(PD-)} / P_{n(mi)}]$ and $\log_2 [P_{n(PD+)} / P_{n(mi)}]$, respectively. These values reflect the efficiency of full-length peptide synthesis for the particular sequence n . The effect of EF-P on suppression of drop-off-reinitiation was evaluated as $W_n = E_{n+} - E_{n-}$. Then, E_{n-} , E_{n+} and W_n of all peptide sequences were summarized and visualized in heat maps (Supplementary Figure S4A–C). Those values were also plotted in histograms (Figure 6C–E, Supplementary Figure S5A, left), in which all peptides were categorized into four groups in terms of the property of amino acids at X_2 , X_3 and X_4 positions [polar residues (DERKHQN), small residues (STGCA), hydrophobic residues (VILMFYW) and Pro (P)].

The average E_n values of peptides bearing Pro at X_2 , X_3 and X_4 were always less than zero regardless of EF-G concentration and presence of EF-P, indicating that Pro at these positions strongly promote drop-off-reinitiation (Figure 6C–E, S5A, left: $E_{n-, X_2=P} = -1.11, -1.28, -1.37$, $E_{n+, X_2=P} = -0.81, -0.78, -1.31$, $E_{n-, X_3=P} = -1.77, -2.00, -2.23$, $E_{n+, X_3=P} = -1.08, -1.70, -2.16$, $E_{n-, X_4=P} = -0.74, -1.15, -1.95$, $E_{n+, X_4=P} = -0.61, -0.60, -1.10$, for 0.03, 0.26 and 10 μM EF-G, respectively). Regarding other types of amino acids than Pro, no significant tendency in average E_n values was observed at positions X_2 and X_3 , whereas at position X_4 polar residues showed significantly lower distribution in E_{n-} , indicating that drop-off-reinitiation is promoted by polar residues at position X_4 in the absence of EF-P (Figure 6C–E: for instance, average $E_{n-} = -0.70, 0.11$ and -0.09 for polar, small and hydrophobic amino acids at 0.26 μM EF-G, average $E_{n-} = -0.94, 0.30$ and 0.10 at 10 μM EF-G). In addition, the difference of average E_{n-} between polar residues and others increased at higher EF-G concentration, showing that EF-G promotes drop-off-reinitiation (Figure 6C–E: ΔE_{n-} for small and hydrophobic residues were -0.83 and -0.40 at 0.03 μM EF-G, -0.81 and -0.61 at 0.26 μM EF-G, -1.24 and -1.04 at 10 μM EF-G). Since E_{n+} at position X_4 did not show any polarity-dependent difference (Figure 6C–E), drop-off-reinitiation can be suppressed by EF-P, which resulted in higher W_n values of polar residues.

In order to confirm the reliability of this profiling system, 6 representative sequences with the highest E_{n-} and 8 sequences with the lowest E_{n-} were individually translated *in vitro* at 10 μM EF-G in the absence or presence of EF-P, and quantified by LC-ESI MS (Supplementary Figure S5B, indicated by black arrows, S5E). The sequences with high E_{n-} could be efficiently translated into full-length peptides along with only a trace amount of reinitiated peptide RiPX even in the absence of EF-P (Supplementary Figure S5F, blue sequences, S5B). On the other hand, the sequences with low E_{n-} could not be translated into full-length at all in the absence of EF-P (Supplementary Figure S5F, orange sequences), but EF-P enabled expression of full-length peptides (Supplementary Figure S5G). We also performed sequence profiling by replacing the triple Pro of the mRNA library with a triple Gly, in which E_{n-} and E_{n+} were less biased than those of the triple-Pro library, and EF-P had no

effect as expected (Supplementary Figure S5A, right, S5D, S4D–F).

In-cell reinitiated peptide synthesis caused by drop-off-reinitiation

Our *in vitro* studies described above undoubtedly have shown that the occurrence of drop-off-reinitiation led to an accumulation of the reinitiated peptide during the translation, so we wondered if this could be observed even in a cellular system. For this study, we chose five *Escherichia coli* proteins, YjgZ, PrpR, YhhM, RutD and YdcO, which have two or three consecutive Pro residues at the N-terminal region. We first set up *in vitro* translation experiments where the respective peptides corresponding to the N-terminal region (14–19 amino acid residues) of these proteins and observed their expression in the absence and presence of EF-P and PTH (Supplementary Figure S6A, FLPN1–5). The respective peptides were radio-labelled with [^{35}S]-methionine (Met or M) at the N-terminus and analyzed by tricine-SDS-PAGE and autoradiography. The bands whose intensities increased in the absence of EF-P and PTH were derived from the dropped peptidyl-tRNA (Supplementary Figure S6B, green arrows). In order to confirm the identities of both DoP and RiP, non-labelled peptides were also expressed in the absence and presence of EF-P (both in the presence of PTH) and subject to LC-ESI MS analysis (Supplementary Figure S6C–G). We observed DoPs originating from peptidyl-tRNA drop-off and RiPs originating from reinitiation at various positions. Notably, expression of FLPN1 (YjgZ), FLPN2 (PrpR) and FLPN4 (RutD) resulted in mainly full-length peptides and relatively small amounts of truncated peptides, whereas FLPN3 (YhhM) and FLPN5 (YdcO) showed severe peptidyl-tRNA drop-off and reinitiation, leading to accumulation of more DoPs and RiPs. Interestingly, in the expression of FLPN5 (MRLFSIPPPTLLAGFLAVL-FLAG), MRLF-SIP was the dominant DoP, indicating that peptidyl-tRNA drop-off mainly occurred at the first Pro residue; However, not PPTLLAGFLAVL-FLAG but PTLLAGFLAVL-FLAG and TLLAGFLAVL-FLAG were the dominant RiPs, indicating that the translation reinitiated from the third Pro or the next Thr by skipping one or two Pro residues. This is probably because the drop-off event occurred successively at the Pro-Pro-Pro sequence.

To this end, we chose YhhM as a model and conducted its cellular expression where FLAG and 6 \times His peptide motifs were added to the C-terminus, referred to as YhhM-fh in order to facilitate the isolation of the full-length as well as reinitiated proteins. This YhhM-fh sequence was cloned into pBAD-HisA vector under the regulation of arabinose promoter. YhhM-fh was expressed in either EF-P-knockout *E. coli* (*E. coli* Δefp) (35,36) or EF-P-expressing *E. coli* bearing modified pBAD vector that complements *efp* gene (Supplementary Figure S7A, *E. coli* $\Delta\text{efp}/+\text{efp}$). In *E. coli* $\Delta\text{efp}/+\text{efp}$, we confirmed $\epsilon(R)$ - β -lysyl-hydroxylation on Lys34 of EF-P, which is introduced by endogenous EpmA/B/C enzymes (37–39) (Supplementary Figure S7B, C). Affinity-purified YhhM-fh was digested by Lys-N (40) and analyzed by LC-ESI MS/MS, by which N-terminal fragments derived from the full-length YhhM-fh and those

lacking 3–5 N-terminal amino acids were detected (Figure 7A, B, Supplementary Figure S6H–U, S8). Note that Lys3 was not cleaved by Lys-N (Figure 7A, B, Supplementary Figure S6H–K, O–R), probably because the N-terminal fMet-Ser prior to Lys3 was too short to be recognized by Lys-N. While the intensity of the Lys-N-digested fragment derived from the full-length YhhM-fh [FLP (fM, M)] was comparable between Δefp and $\Delta\text{efp}/+\text{efp}$ (Figure 7C, the relative intensities were $4.9 \pm 1.1 \times 10^4$ and $11 \pm 6 \times 10^4$, respectively; Figure 7D, their fractions were $93 \pm 3\%$ and $99 \pm 4\%$, respectively), the intensity of the RiP fragment lacking fMet-Ser-Lys-Pro-Pro (RiP Δ N3) was higher in Δefp than in $\Delta\text{efp}/+\text{efp}$ (Figure 7C, their relative intensities were $3.1 \pm 0.9 \times 10^3$ and $6 \pm 4 \times 10^2$, respectively, with $P < 0.05$ in Welch's *t* test; Figure 7D, their fractions were $6 \pm 3\%$ and $0.5 \pm 0.3\%$, respectively, with $P < 0.1$ in Welch's *t* test). This result suggests that the drop-off-reinitiation event occurred more frequently in the absence of EF-P than its presence because of inefficient peptidyl transfer. Among a series of RiP fragments lacking several N-terminal amino acids, RiP Δ N3 was clearly dominant, indicating that the peptidyl transfer between peptidyl-diproyl-tRNA and leucyl-tRNA was inefficient in the expression of YhhM-fh in the absence of EF-P (Figure 7C, the relative intensity of RiP Δ N1, 2 and 3 expressed in the absence of EF-P was $1.6 \pm 1.2 \times 10^2$, $0.8 \pm 0.3 \times 10^2$ and $3.1 \pm 0.9 \times 10^3$, respectively, while those in the presence of EF-P was $1.5 \pm 1.5 \times 10^2$, $1.4 \pm 0.9 \times 10^2$ and $6 \pm 4 \times 10^2$, respectively; Figure 7D, the fractions of RiP Δ N1, 2 and 3 expressed in the absence of EF-P were $0.3 \pm 0.2\%$, $0.15 \pm 0.05\%$ and $6 \pm 3\%$, respectively, while those in the presence of EF-P was $0.2 \pm 0.1\%$, $0.12 \pm 0.07\%$ and $0.5 \pm 0.3\%$, respectively).

In this cell-based assay, an overexpressed protein, YhhM-fh, was analyzed because the use of a specific tag sequence was necessary for the efficient isolation and detection of the fragments. However, the result has strongly supported a possibility where the drop-off-reinitiation could occur in the cellular system. The evolutionary importance of EF-P is also supported by this result, in turn suggesting why EF-P and its homologs are widely conserved in the three domains of life. Thus, the drop-off-reinitiation can frequently occur without EF-P, resulting in an accumulation of aberrant proteins that lack their N-terminal region.

DISCUSSION

Although the mechanism and processing pathway of peptidyl-tRNA drop-off event have been previously studied (2–4), the fate of the ribosome complex that lost the peptidyl-tRNA has not been well understood. Here, we reported for the first time that such a ribosome complex is subject to EF-G-dependent translocation and then reinitiation occurs to yield an RiP (Figure 8B). We referred this event to as drop-off-reinitiation and confirmed that it occurs both *in vitro* and in cells. The frequency of drop-off-reinitiation is regulated by the following two factors: (i) translocation frequency and (ii) peptidyl transfer efficiency (Figure 8C).

EF-G is the critical regulator that determines translocation frequency (Figure 8C left). In the canonical translo-

cation, EF-G mediates migration of P/E-site deacylated-tRNA and A/P-site peptidyl-tRNA in the hybrid state to E/E and P/P site, respectively, after completion of peptidyl transfer (Figure 8A) (17). In contrast, in the mistranslocation, P/P-site peptidyl-tRNA and A/A-site aminoacyl-tRNA migrate toward E/E and P/P site, respectively, before peptidyl transfer completes (Figure 8B). It has been previously reported that N-acetyl-Phe-tRNA in the P site can translocate toward E site, albeit less efficiently than the canonical translocation (41). Presumably, the nascent peptide on the peptidyl-tRNA perturbs the interaction between the tRNA and 23S rRNA in the E site and thereby makes the translocation less efficient (42,43). It has been also reported that a replacement of the peptidyl group of A-site tRNA with an aminoacyl group inhibits the translocation to P site (44). Moreover, since EF-G should bind preferably to the rotated ribosome/tRNAs in the hybrid state compared to those in the non-rotated classical state, the mistranslocation would not efficiently take place at a low concentration of EF-G. Therefore, an elevation of the EF-G concentration should be required to induce the mistranslocation with a higher frequency, yielding more RiPs. The concentration of EF-G in *E. coli* cell is estimated to be approximately twofold higher than that of 70S ribosome (45), which corresponds to $2.4 \mu\text{M}$ in the case of our *in vitro* translation system whose concentration of ribosome is $1.2 \mu\text{M}$. In this EF-G concentration range, peptidyl-tRNA drop-off is induced but suppressed by EF-P *in vitro* (Figure 1B). A similar trend was observed in the in-cell experiment, in which the YhhM-fh lacking its N-terminus was detected but largely suppressed by EF-P.

Susceptibility of P-site peptidyl-tRNA to drop-off is another regulator of the drop-off-reinitiation frequency (Figure 8C left). Shorter nascent peptides of peptidyl-tRNA increased the drop-off susceptibility due to the insufficient interaction with the exit tunnel, and resulted in more RiP synthesis (Figure 4). In *E. coli* cells, there are 2115 proteins and putative proteins containing two or more consecutive Pro, 6% of which are located within N-terminal 24 amino acid residues (46). When the nascent peptide on peptidyl-Pro-tRNA is shorter than the depth of the exit tunnel, RiP synthesis possibly tends to occur via drop-off-reinitiation. If that is the case, the population of RiPs should not be ignorable, although more comprehensive in-cell studies should be performed to verify this.

As for the regulators of peptidyl transfer efficiency (Figure 8C right), we evaluated the effect of consecutive Pro residues in model peptides and proteins. Increasing the number of consecutive Pro, RiPs derived from mistranslocation were more frequently observed. The inefficient peptidyl transfer observed for the consecutive Pro elongation can be alleviated by adding EF-P to the translation system, by which drop-off-reinitiation was also suppressed. EF-P recognizes the P-site peptidyl-Pro-tRNA^{Pro} and stabilizes its CCA end for shaping suitable geometry for peptidyl transfer (47). In addition to consecutive Pro, certain nascent peptide sequences that interact with the ribosomal exit tunnel also make peptidyl transfer inefficient. We conducted a comprehensive analysis of 8,420 nascent peptide sequences preceding the three consecutive Pro, showing that polar amino acids adjacent to the Pro stretch significantly

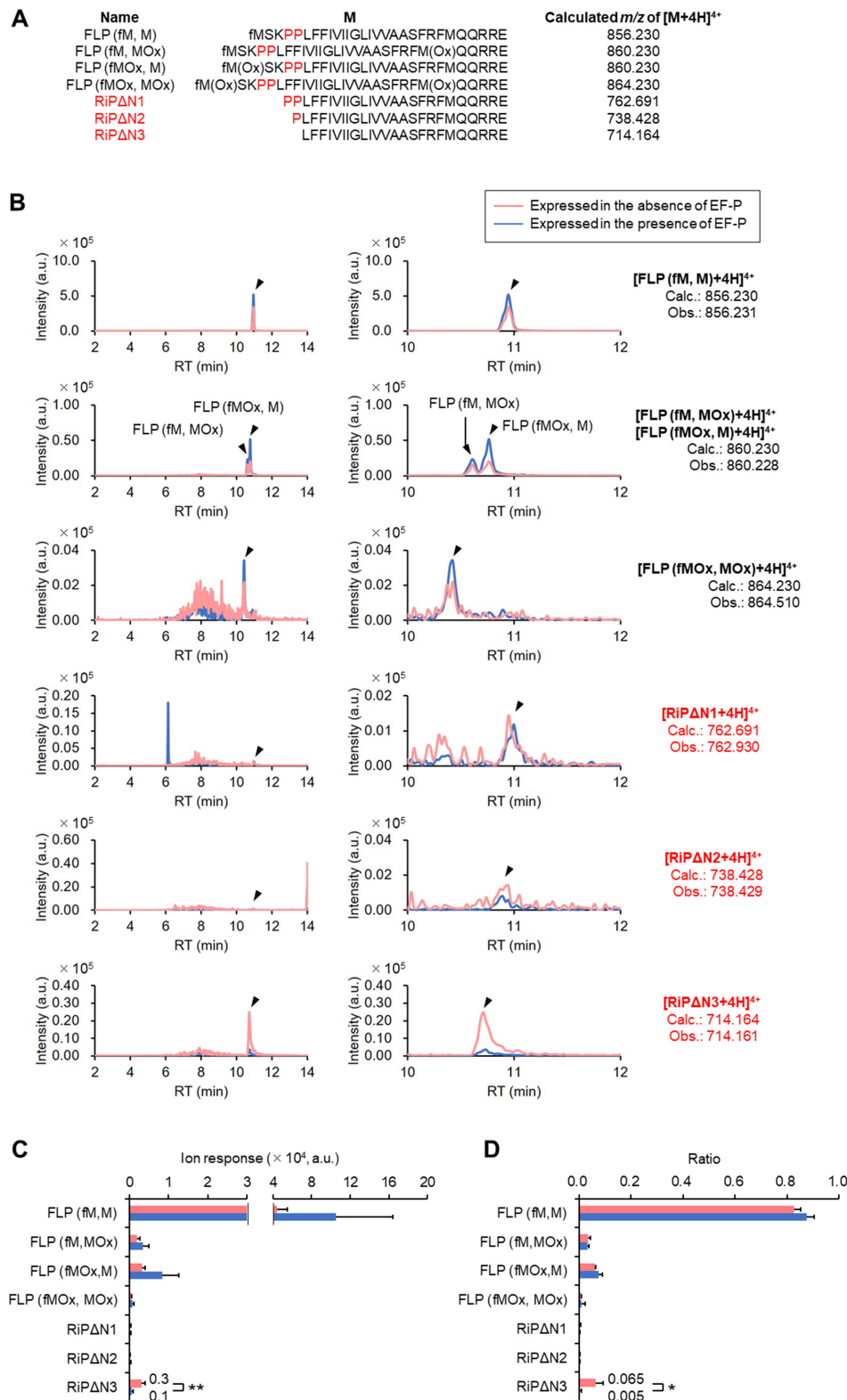


Figure 7. LC-ESI MS analysis of N-terminal fragments of YhhM-fh expressed in *E. coli*. (A) N-terminal peptide sequences generated by Lys-N digestion of full-length YhhM-fh (FLP) and reinitiated YhhM-fh lacking its N-terminal amino acids (RiPΔN1, RiPΔN2 and RiPΔN3). MOx: Methionine oxidized on its sidechain thioether. (B) Full-range (left) and magnified (right) XICs of N-terminal peptides generated by Lys-N digestion of YhhM-fh expressed alone (red) and co-expressed with EF-P (blue). XICs were extracted on the observed m/z values (Obs.). (C, D) LC-ESI MS quantification of ion response (C) and ratio (D) of N-terminal fragments generated by Lys-N digestion of YhhM-fh expressed in the absence or presence of EF-P. Ratios were calculated as (ion response of an N-terminal fragment)/(sum of ion responses of all the N-terminal fragments). SD of three independent experiments using YhhM-fh expressed without EF-P and SD of four independent experiments using YhhM-fh expressed with EF-P are shown. * $P < 0.1$ in Welch's t test. ** $P < 0.05$ in Welch's t test.

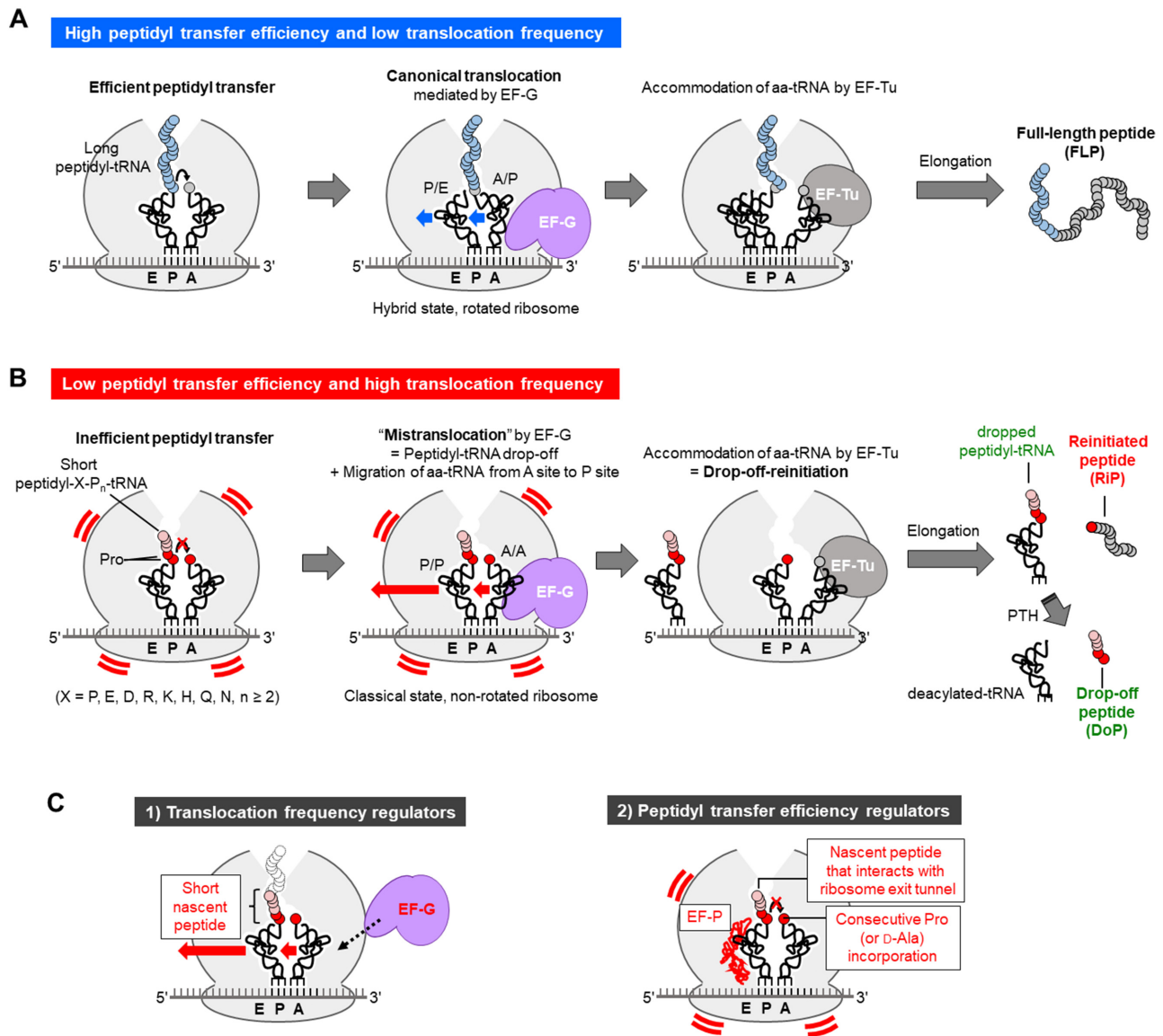


Figure 8. Overview of EF-G-driven mistranslocation and drop-off-reinitiation. (A) Schematic illustration of peptide elongation in the canonical translation. Ribosome catalyzes peptidyl transfer by which a new peptide bond is formed between a nascent peptide on P-site peptidyl-tRNA (blue) and an amino acid on A-site aminoacyl-tRNA (grey). In the canonical translocation mediated by EF-G (purple), P-site deacylated-tRNA and A-site peptidyl-tRNA migrate to E site and P site, respectively. In accommodation, an aminoacyl-tRNA corresponding to the next A-site codon is delivered by EF-Tu. By repeating the three reactions, a full-length peptide is synthesized. (B) Schematic illustration of P-site peptidyl-tRNA drop-off and generation of reinitiated peptide caused by mistranslocation and drop-off-reinitiation. Consecutive incorporation of prolines (P, red) makes peptidyl transfer reaction inefficient. Before completion of the inefficient peptidyl transfer, drop-off of the peptidyl-tRNA and migration of A-site aminoacyl-tRNA to P site occur, which we refer to as mistranslocation. Then, translation is reinitiated by accommodation of a new aminoacyl-tRNA on to A site to give a reinitiated peptide, RiP. (C) Candidates of translocation frequency regulators (1, left) and peptidyl transfer frequency regulators (2, right). Those indicated by red letters are confirmed translocation frequency regulators (short nascent peptide and EF-G) and peptidyl transfer frequency regulators (consecutive Pro incorporation, EF-P and sequence of nascent peptide).

promoted drop-off-reinitiation, which was also suppressed by EF-P (Figure 6, Supplementary Figure S4A–C). Our result looks consistent with previous related studies where Pro and polar amino acids, such as Arg, Asp, His and Lys, were preferred at position X of the stalling motif, XPP or XPPP, although the contribution of polar residues was not clearly discussed in the papers (48–50). These studies also showed that the sequence dependent ribosome stalling was alleviated by EF-P. Not only consecutive Pro motifs but

also other types of arrest peptides and ribosome destabilizing peptides have also been reported. For example, expression of TnaC stalls with the P-site peptidyl-Pro-tRNA (51), whereas that of SecM stalls with the A-site Pro-tRNA (52). MgtL peptide (MEPDPTPLPRRLKLF) and peptides bearing 10 consecutive acidic residues also destabilize ribosome upon Mg^{2+} starvation, leading to a dissociation of the ribosomal subunits and eventually translation abortion (53). Although the mechanisms for the ribosomal

stalling and destabilization are not fully understood, both Pro and polar/acidic residues in such peptides may force the peptidyl-tRNA inactive for peptidyl transfer reaction by electrostatic repulsion with the tunnel. Therefore, these peptide sequences also act as potent drop-off-reinitiation inducers (Figure 8C right).

Drop-off-reinitiation induced by mistranslocation is distinct from other ribosome rescue pathways mediated by specific quality control factors, such as tmRNA/SmpB (54,55), ArfA (56) and ArfB (57). These rescue pathways do not generate RiPs from the stalled ribosome. Since both A and P sites are occupied by peptidyl- and aminoacyl-tRNAs, respectively, in the case of drop-off-reinitiation, these rescue factors cannot enter the A site where they work. Although we could detect RiPs in *E. coli*, it is still unclear whether such truncated peptides/proteins are rapidly and selectively degraded or can circumvent such degradation pathway to survive. If the N-end rule pathway applies to the truncated proteins (58), the lack of fMet and the alternate N-terminal amino acids (typically Pro) would play a role in protein stability. Elucidation of these issues should be important for future works.

SUPPLEMENTARY DATA

Supplementary Data are available at NAR Online.

ACKNOWLEDGEMENTS

We thank to the National BioResource Project-*E. coli* at National Institute of Genetics (NBRP-*E. coli* at NIG) for the distribution of efp-knocked-out *E. coli* strain. We thank Dr Naoya Ozawa for writing a Python code to analyze DNA sequence data.

FUNDING

Human Frontier Science Program [RGP0015/2017 to H.S.]; Japan Society for the Promotion of Science (JSPS) Grant-in-Aid for Scientific Research (B) [18H02080 to T.K.]; Grants-in-Aid for JSPS Fellows [18J12342 to K.T.]. Funding for open access charge: Society for the Promotion of Science (JSPS) Grant-in-Aid for Scientific Research (B) [18H02080].

Conflict of interest statement. None declared.

REFERENCES

- Schmeing, T.M. and Ramakrishnan, V. (2009) What recent ribosome structures have revealed about the mechanism of translation. *Nature*, **461**, 1234–1242.
- Menninger, J.R. (1976) Peptidyl transfer RNA dissociates during protein synthesis from ribosomes of *Escherichiacoli*. *J. Biol. Chem.*, **251**, 3392–3398.
- Cruz-Vera, L.R., Magos-Castro, M.A., Zamora-Romo, E. and Guarneros, G. (2004) Ribosome stalling and peptidyl-tRNA drop-off during translational delay at AGA codons. *Nucleic Acids Res.*, **32**, 4462–4468.
- de Valdivia, E.I.G. and Isaksson, L.A. (2005) Abortive translation caused by peptidyl-tRNA drop-off at NGG codons in the early coding region of mRNA. *FEBS J.*, **272**, 5306–5316.
- Fujino, T., Goto, Y., Suga, H. and Murakami, H. (2013) Reevaluation of the D-amino acid compatibility with the elongation event in translation. *J. Am. Chem. Soc.*, **135**, 1830–1837.
- Muto, H. and Ito, K. (2008) Peptidyl-prolyl-tRNA at the ribosomal P-site reacts poorly with puromycin. *Biochem. Biophys. Res. Commun.*, **366**, 1043–1047.
- Doerfel, L.K., Wohlgenuth, I., Kothe, C., Peske, F., Urlaub, H. and Rodnina, M.V. (2013) EF-P is essential for rapid synthesis of proteins containing consecutive proline residues. *Science*, **339**, 85–88.
- Ude, S., Lassak, J., Starosta, A.L., Kraxenberger, T., Wilson, D.N. and Jung, K. (2013) Translation elongation factor EF-P alleviates ribosome stalling at polyproline stretches. *Science*, **339**, 82–85.
- Pavlov, M.Y., Watts, R.E., Tan, Z., Cornish, V.W., Ehrenberg, M. and Forster, A.C. (2009) Slow peptide bond formation by proline and other N-alkylamino acids in translation. *Proc. Natl. Acad. Sci. U.S.A.*, **106**, 50–54.
- Otaka, T. and Kaji, A. (1975) Release of (oligo) peptidyl-tRNA from ribosomes by erythromycin A. *Proc. Natl. Acad. Sci. U.S.A.*, **72**, 2649–2652.
- Menninger, J.R. and Otto, D.P. (1982) Erythromycin, carbomycin, and spiramycin inhibit protein synthesis by stimulating the dissociation of peptidyl-tRNA from ribosomes. *Antimicrob. Agents Chemother.*, **21**, 811–818.
- Lovmar, M., Tenson, T. and Ehrenberg, M. (2004) Kinetics of macrolide action. *J. Biol. Chem.*, **279**, 53506–53515.
- Tenson, T., Lovmar, M. and Ehrenberg, M. (2003) The mechanism of action of macrolides, lincosamides and streptogramin B reveals the nascent peptide exit path in the ribosome. *J. Mol. Biol.*, **330**, 1005–1014.
- Mankin, A.S. (2008) Macrolide myths. *Curr. Opin. Microbiol.*, **11**, 414–421.
- Das, G. and Varshney, U. (2006) Peptidyl-tRNA hydrolase and its critical role in protein biosynthesis. *Microbiology*, **152**, 2191–2195.
- Kang, T.J. and Suga, H. (2011) Translation of a histone H3 tail as a model system for studying peptidyl-tRNA drop-off. *FEBS Lett.*, **585**, 2269–2274.
- Rodnina, M.V., Savelsbergh, A., Katunin, V.I. and Wintermeyer, W. (1997) Hydrolysis of GTP by elongation factor G drives tRNA movement on the ribosome. *Nature*, **385**, 37–41.
- Gao, Y.G., Selmer, M., Dunham, C.M., Weixlbaumer, A., Kelley, A.C. and Ramakrishnan, V. (2009) The structure of the ribosome with elongation factor G trapped in the posttranslocational state. *Science*, **326**, 694–699.
- Saito, H., Kourouklis, D. and Suga, H. (2001) An *in vitro* evolved precursor tRNA with aminoacylation activity. *EMBO J.*, **20**, 1797–1806.
- Murakami, H., Ohta, A., Ashigai, H. and Suga, H. (2006) A highly flexible tRNA acylation method for non-natural polypeptide synthesis. *Nat. Methods*, **3**, 357–359.
- Johansson, M., Jeong, K.W., Trobro, S., Strazewski, P., Åqvist, J., Pavlov, M.Y. and Ehrenberg, M. (2011) pH-sensitivity of the ribosomal peptidyl transfer reaction dependent on the identity of the A-site aminoacyl-tRNA. *Proc. Natl. Acad. Sci. U.S.A.*, **108**, 79–84.
- Tanner, D.R., Cariello, D.A., Woolstenhulme, C.J., Broadbent, M.A. and Buskirk, A.R. (2009) Genetic identification of nascent peptides that induce ribosome stalling. *J. Biol. Chem.*, **284**, 34809–34818.
- Heurgué-Hamard, V., Karimi, R., Mora, L., MacDougall, J., Leboeuf, C., Grentzmann, G., Ehrenberg, M. and Buckingham, R.H. (1998) Ribosome release factor RF4 and termination factor RF3 are involved in dissociation of peptidyl-tRNA from the ribosome. *EMBO J.*, **17**, 808–816.
- Gong, M., Cruz-Vera, L.R. and Yanofsky, C. (2007) Ribosome recycling factor and release factor 3 action promotes TnaC-peptidyl-tRNA dropoff and relieves ribosome stalling during tryptophan induction of tna operon expression in *Escherichiacoli*. *J. Bacteriol.*, **189**, 3147–3155.
- Singh, N.S., Ahmad, R., Sangeetha, R. and Varshney, U. (2008) Recycling of ribosomal complexes stalled at the step of elongation in *Escherichia coli*. *J. Mol. Biol.*, **380**, 451–464.
- Katoh, T., Wohlgenuth, I., Nagano, M., Rodnina, M.V. and Suga, H. (2016) Essential structural elements in tRNA^{Pro} for EF-P-mediated alleviation of translation stalling. *Nat. Commun.*, **7**, 11657.
- Alejo, J.L. and Blanchard, S.C. (2017) Miscoding-induced stalling of substrate translocation on the bacterial ribosome. *Proc. Natl. Acad. Sci. U.S.A.*, **114**, E8603–E8610.

28. Gamper, H.B., Masuda, I., Frenkel-Morgenstern, M. and Hou, Y.M. (2015) Maintenance of protein synthesis reading frame by EF-P and m¹G37-tRNA. *Nat. Commun.*, **6**, 7226.
29. Vogel, Z., Vogel, T., Zamir, A. and Elson, D. (1971) The protection by 70 S ribosomes of N-acyl-aminoacyl-tRNA against cleavage by peptidyl-tRNA hydrolase and its use to assay ribosomal association. *Eur. J. Biochem.*, **21**, 582–592.
30. Ito, K. and Chiba, S. (2013) Arrest peptides: cis-acting modulators of translation. *Annu. Rev. Biochem.*, **82**, 171–202.
31. Li, G.W., Oh, E. and Weissman, J.S. (2012) The anti-Shine-Dalgarno sequence drives translational pausing and codon choice in bacteria. *Nature*, **484**, 538–541.
32. Mohammad, F., Woolstenhulme, C.J., Green, R. and Buskirk, A.R. (2016) Clarifying the translational pausing landscape in bacteria by ribosome profiling. *Cell Rep.*, **14**, 686–694.
33. Goto, Y., Katoh, T. and Suga, H. (2011) Flexizymes for genetic code reprogramming. *Nat. Protoc.*, **6**, 779–790.
34. Rogers, J.M., Passioura, T. and Suga, H. (2018) Nonproteinogenic deep mutational scanning of linear and cyclic peptides. *Proc. Natl. Acad. Sci. U.S.A.*, **115**, 10959–10964.
35. Baba, T., Ara, T., Hasegawa, M., Takai, Y., Okumura, Y., Baba, M., Datsenko, K.A., Tomita, M., Wanner, B.L. and Mori, H. (2006) Construction of *Escherichiacoli* K-12 in-frame, single-gene knockout mutants: the Keio collection. *Mol. Syst. Biol.*, **2**, 2006.0008.
36. Yamamoto, N., Nakahigashi, K., Nakamichi, T., Yoshino, M., Takai, Y., Touda, Y., Furubayashi, A., Kinjyo, S., Dose, H., Hasegawa, M. et al. (2009) Update on the Keio collection of *Escherichiacoli* single-gene deletion mutants. *Mol. Syst. Biol.*, **5**, 335.
37. Roy, H., Zou, S.B., Bullwinkle, T.J., Wolfe, B.S., Gilreath, M.S., Forsyth, C.J., Navarre, W.W. and Ibba, M. (2011) The tRNA synthetase paralog PoxA modifies elongation factor-P with (R)- β -lysine. *Nat. Chem. Biol.*, **7**, 667–669.
38. Yanagisawa, T., Sumida, T., Ishii, R., Takemoto, C. and Yokoyama, S. (2010) A paralog of lysyl-tRNA synthetase aminoacylates a conserved lysine residue in translation elongation factor P. *Nat. Struct. Mol. Biol.*, **17**, 1136–1143.
39. Peil, L., Starosta, A.L., Virumäe, K., Atkinson, G.C., Tenson, T., Remme, J. and Wilson, D.N. (2012) Lys34 of translation elongation factor EF-P is hydroxylated by YfcM. *Nat. Chem. Biol.*, **8**, 695–697.
40. Nonaka, T., Hashimoto, Y. and Takio, K. (1998) Kinetic characterization of lysine-specific metalloendopeptidases from *Grifolafrondosa* and *Pleurotostreatus* fruiting bodies. *J. Biochem.*, **124**, 157–162.
41. Fredrick, K. and Noller, H.F. (2002) Accurate translocation of mRNA by the ribosome requires a peptidyl group or its analog on the tRNA moving into the 30S P site. *Mol. Cell*, **9**, 1125–1131.
42. Lill, R., Lepier, A., Schwägele, F., Sprinzl, M., Vogt, H. and Wintermeyer, W. (1988) Specific recognition of the 3'-terminal adenosine of tRNA^{Phe} in the exit site of *Escherichia coli* ribosomes. *J. Mol. Biol.*, **203**, 699–705.
43. Lill, R., Robertson, J.M. and Wintermeyer, W. (1989) Binding of the 3' terminus of tRNA to 23S rRNA in the ribosomal exit site actively promotes translocation. *EMBO J.*, **8**, 3933–3938.
44. Walker, S.E., Shoji, S., Pan, D., Cooperman, B.S. and Fredrick, K. (2008) Role of hybrid tRNA-binding states in ribosomal translocation. *Proc. Natl. Acad. Sci. U.S.A.*, **105**, 9192–9197.
45. Schmidt, A., Kochanowski, K., Vedelaar, S., Ahrné, E., Volkmer, B., Callipo, L., Knoops, K., Bauer, M., Aebersold, R. and Heinemann, M. (2016) The quantitative and condition-dependent *Escherichia coli* proteome. *Nat. Biotechnol.*, **34**, 104–110.
46. Qi, F., Motz, M., Jung, K., Lassak, J. and Frishman, D. (2018) Evolutionary analysis of polyproline motifs in *Escherichia coli* reveals their regulatory role in translation. *PLoS Comput. Biol.*, **14**, e1005987.
47. Huter, P., Arenz, S., Bock, L.V., Graf, M., Frister, J.O., Heuer, A., Peil, L., Starosta, A.L., Wohlgemuth, I., Peske, F. et al. (2017) Structural basis for polyproline-mediated ribosome stalling and rescue by the translation elongation factor EF-P. *Mol. Cell*, **68**, 515–527.
48. Peil, L., Starosta, A.L., Lassak, J., Atkinson, G.C., Virumäe, K., Spitzer, M., Tenson, T., Jung, K., Remme, J. and Wilson, D.N. (2013) Distinct XPPX sequence motifs induce ribosome stalling, which is rescued by the translation elongation factor EF-P. *Proc. Natl. Acad. Sci. U.S.A.*, **110**, 15265–15270.
49. Starosta, A.L., Lassak, J., Peil, L., Atkinson, G.C., Virumäe, K., Tenson, T., Remme, J., Jung, K. and Wilson, D.N. (2014) Translational stalling at polyproline stretches is modulated by the sequence context upstream of the stall site. *Nucleic Acids Res.*, **42**, 10711–10719.
50. Woolstenhulme, C.J., Guydosh, N.R., Green, R. and Buskirk, A.R. (2015) High-precision analysis of translational pausing by ribosome profiling in bacteria lacking EFP. *Cell Rep.*, **11**, 13–21.
51. Gong, F., Ito, K., Nakamura, Y. and Yanofsky, C. (2001) The mechanism of tryptophan induction of tryptophanase operon expression: tryptophan inhibits release factor-mediated cleavage of TnaC-peptidyl-tRNA^{Pro}. *Proc. Natl. Acad. Sci. U.S.A.*, **98**, 8997–9001.
52. Nakatogawa, H. and Ito, K. (2001) Secretion monitor, secM, undergoes self-translation arrest in the cytosol. *Mol. Cell*, **7**, 185–192.
53. Chadani, Y., Niwa, T., Izumi, T., Sugata, N., Nagao, A., Suzuki, T., Chiba, S., Ito, K. and Taguchi, H. (2017) Intrinsic ribosome destabilization underlies translation and provides an organism with a strategy of environmental sensing. *Mol. Cell*, **68**, 528–539.
54. Keiler, K.C., Waller, P.R.H. and Sauer, R.T. (1996) Role of a peptide tagging system in degradation of proteins synthesized from damaged messenger RNA. *Science*, **271**, 990–993.
55. Karzai, A.W., Susskind, M.M. and Sauer, R.T. (1999) SmpB, a unique RNA-binding protein essential for the peptide-tagging activity of SsrA (tmRNA). *EMBO J.*, **18**, 3793–3799.
56. Chadani, Y., Ono, K., Ozawa, S., Takahashi, Y., Takai, K., Nanamiya, H., Tozawa, Y., Kutsukake, K. and Abo, T. (2010) Ribosome rescue by *Escherichia coli* ArfA (YhdL) in the absence of trans-translation system. *Mol. Microbiol.*, **78**, 796–808.
57. Chadani, Y., Ono, K., Kutsukake, K. and Abo, T. (2011) *Escherichia coli* YaeJ protein mediates a novel ribosome-rescue pathway distinct from SsrA- and ArfA-mediated pathways. *Mol. Microbiol.*, **80**, 772–785.
58. Dougan, D.A., Truscott, K.N. and Zeth, K. (2010) The bacterial N-end rule pathway: expect the unexpected. *Mol. Microbiol.*, **76**, 545–558.